

Fig. 1. Phylogenetic tree of the partial RNA polymerase region of the HEV genome. Twenty-four genotype 3 and 24 genotype 4 strains in Japan showed each significant cluster to have a high bootstrap value and to be distinct from other reference sequences (USA, Canada and Japanese minor strains in genotype 3; Chinese strains in genotype 4). Genetic distances have been transformed into a time scale of years by using estimates of the molecular clock (0.84×10^{-3} nucleotide substitutions per site year⁻¹). Ten strains in bold are used for linear regression in Fig. 2. Strain names are followed by prefecture or city names in Japan: Tok, Tokyo; Sai, Saitama; Sap, Sapporo; Iwa, Iwate; Kan, Kanagawa; Oki, Okinawa; Aom, Aomori; Nar, Nara; Tot, Tottori; Nii, Niigata; Toc, Tochigi; Toy, Toyama. Asterisks indicate strains that were newly sequenced in this study.

Japan. In this study, we first estimated the evolutionary rate of HEV by using Japan-indigenous genotype 3 and genotype 4 strains, which were phylogenetically distinct from the other strains in foreign countries. Then, based on this evolutionary rate, we traced the demographic history of HEV in Japan.

For linear-regression analyses within significant clusters, two independent datasets were applied: one was a Hyogo cluster (genotype 3) with JMO-Hyo03L, JTH-Hyo03L, JSO-Hyo03L, JYO-Hyo03L, JDEER-Hyo03L (these five isolates were obtained in April 2003) and JBOAR1-Hyo04 (April 2004) (Takahashi *et al.*, 2004a), and another was a Sapporo cluster (genotype 4) with JSM-Sap95 (March 1995), JKK-Sap00 (November 2000), JYWSap02 (August 2002) and

JTS-Sap02 (September 2002) (Takahashi *et al.*, 2004b). GenBank accession numbers for these strains are given in Fig. 1. To elucidate the epidemiological history of the HEV population in Japan, 48 known and newly sequenced HEV strains ($n=24$ for each of genotype 3 and 4) were used for molecular-evolutionary analyses. The nucleotide sequences of 28 strains for the molecular-clock analyses were determined in this study (the other 20 sequences dealt with in this paper were available from GenBank).

Nucleic acids were extracted from serum samples (50 µl) by using a commercial Smitest EX-R & D kit (Genome Science) and precipitated in a 2 ml tube. The pellet was air-dried for 15 min and then suspended in 10 µl autoclaved distilled water containing 10 U RNase inhibitor ml⁻¹ (TaKaRa

Shuzo). A sequence spanning 821 nt in the RNA-dependent RNA polymerase region (corresponding to nt 3961–4781 of the prototype Burmese HEV strain; GenBank accession no. M73218), including the GDD motif, was amplified by PCR in three overlapping regions with 20-mer primers deduced from known HEV sequences. Reverse transcription was performed at 50 °C for 60 min with the Thermo-Script RT system (Invitrogen), and the first- and second-round PCRs were carried out in the presence of Platinum *Taq* DNA Polymerase High Fidelity (Invitrogen). The final products were sequenced in an ABI 377 DNA sequencer (PE Biosystems) with an ABI Prism BigDye kit (Applied Biosystems). The sequences determined were utilized to confirm HEV genotypes and to construct phylogenetic trees. The reliability of the phylogenetic tree was assessed by bootstrap-resampling tests.

A reconstructed tree was built on the RNA polymerase region by using a heuristic maximum-likelihood (ML) topology search with stepwise addition and nearest neighbour-interchange algorithms. Tree likelihood scores were calculated by using the HKY85 model (Hasegawa *et al.*, 1985) with the molecular clock enforced, using PAUP version 4.0b8. Using the estimated topology, all possible root positions were evaluated under a single-rate dated-tips (SRDT) model with the computer software TipDate v1.2 and the root that yielded the highest likelihood was adopted (Rambaut, 2000). The program provided an ML estimate of the rate and also the associated date of the most recent common ancestor of the sequences, using a model that assumed a constant rate of nucleotide substitution. The molecular clock was tested by a likelihood-ratio test between the SRDT model and a general unconstrained branch-length model [different-rate (DR) model].

For estimates of demographic history, a non-parametric function $N(t)$, also known as a skyline plot, was obtained by transforming the coalescent intervals of an observed genealogy into a piecewise plot that represented an effective population size through time (Pybus *et al.*, 2001; Pybus & Rambaut, 2002). A parametric ML was estimated by several models with the computer software GENIE v3.5 to build a statistical framework for inferring the demographic history of a population on phylogenies reconstructed from sampled DNA sequences (Pybus & Rambaut, 2002). This model assumes a continuous epidemic process in which the viral transmission parameters remain constant through time. Model fitting was evaluated by likelihood-ratio tests of the parametric ML estimates (Lemey *et al.*, 2003; Pybus *et al.*, 2003; Tanaka *et al.*, 2005). Approximate 95 % confidence intervals for the parameters were estimated by using the likelihood-ratio test statistics.

A phylogenetic tree in the partial RNA polymerase region of the HEV genome is represented in Fig. 1. A functional gene, such as the RNA polymerase gene, is suitable for molecular-evolutionary analyses based on the neutral theory, because the substitution of functional genes is based on the neutral theory. The 24 genotype 3 and 24 genotype 4 strains in Japan

showed a significant cluster with a high bootstrap value, which was the major Japanese cluster distinct from other strains found in foreign countries by molecular-evolutionary analyses. Such a significant cluster is suitable for the following coalescent analysis. Additionally, the tree topology based on the RNA polymerase region, including functional genes, was quite similar to that based on complete genomes (data not shown).

To determine the evolutionary rate of HEV, the 48 Japan-indigenous HEV strains (Fig. 1) were subjected to further molecular-evolutionary analyses. The molecular-evolutionary rate was estimated by two independent methods. In brief, linear-regression analyses using highly similar strains, i.e. six genotype 3 strains in Hyogo and four genotype 4 strains in Sapporo, indicated that a molecular-evolutionary rate was $(0.81\text{--}0.88) \times 10^{-3}$ nucleotide substitutions per site year⁻¹ (Fig. 2). Second, TipDate (v1.2) was used to compare the DR model with the single-rate (SR) and SRDT models. The SRDT model provided an adequate fit to the data ($P > 0.05$; see Supplementary Table S1, available in JGV Online). Based on the SRDT model, the mean rate of nucleotide substitutions was estimated to be $(0.81\text{--}0.94) \times 10^{-3}$ nucleotide

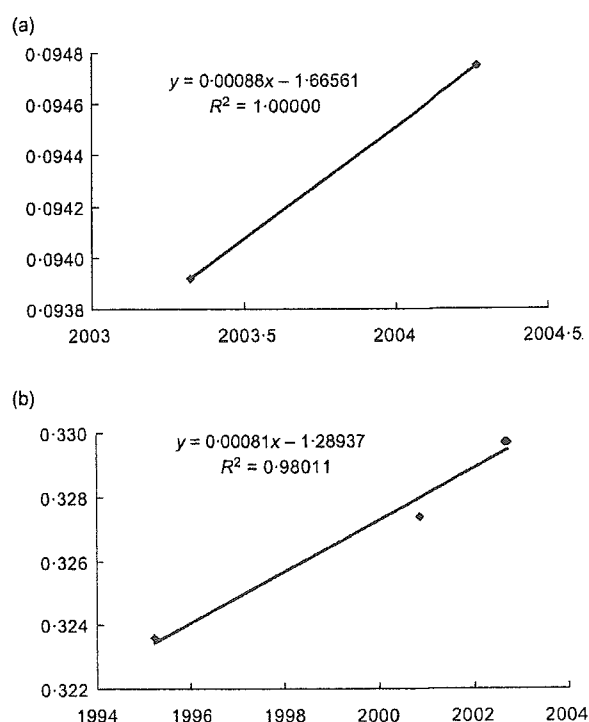


Fig. 2. Linear-regression analyses within the partial RNA polymerase region for evolutionary rate of HEV. (a) The evolutionary rate of genotype 3 in the Hyogo cluster is estimated to be 0.88×10^{-3} nucleotide substitutions per site year⁻¹; (b) the evolutionary rate of genotype 4 in the Sapporo cluster is estimated to be 0.81×10^{-3} nucleotide substitutions per site year⁻¹.

substitutions per site year⁻¹, which was similar to the rate for *Hepatitis C virus* (Ina *et al.*, 1994; Tanaka *et al.*, 2002). When we used 0.84×10^{-3} nucleotide substitutions per site year⁻¹, which was based on all 48 sequences (24 genotype 3 and 24 genotype 4), the time of the most recent common ancestor of Japan-indigenous genotype 3 was estimated to be in the 1900s (95 % confidence interval, 1902–1917) and that of genotype 4 was approximately in the 1880s (1881–1898) (Fig. 1).

Based on the phylogenetic tree, the effective number of HEV infections through time, $N(t)$, was analysed by using a skyline plot for the Japan-indigenous HEV strains. The parameters for several models in GENIE v3.5 were examined (see Supplementary Table S2, available in JGV Online). Time t was then transformed to year by using the constant rate (0.84×10^{-3} nucleotide substitutions per site year⁻¹), assuming the collecting time to be the present. Fig. 3 shows the skyline plots and population growth for the HEV strains, according to a specific demographic model in GENIE v3.5

with three parameters and a piecewise-expansion growth model, which was evaluated by likelihood-ratio testing (Ina *et al.*, 1994; Lemey *et al.*, 2003; Pybus *et al.*, 2003; Tanaka *et al.*, 2005). Our estimates of the effective numbers of HEV infections showed a transition from constant size to exponential growth in the 1920s (95 % confidence interval, 1916–1930) among the genotype 3 population (Fig. 3a), whereas the rapid exponential growth among the genotype 4 population was dated in the 1980s (1978–1990) (Fig. 3b).

Because the natural course of HEV infection in human beings and animals is usually transient, not persistent as in the cases of hepatitis B and C viruses, it is almost impossible to estimate the molecular-evolutionary rate of HEV by using serial samples from an individual host. However, even though HEV does not persist in individual hosts, it could persist in the community by hopping from host to host successively. The first study attempting to estimate the number of synonymous mutations per synonymous site (k_s) of *Hepatitis A virus* (HAV) was reported by Sánchez *et al.*

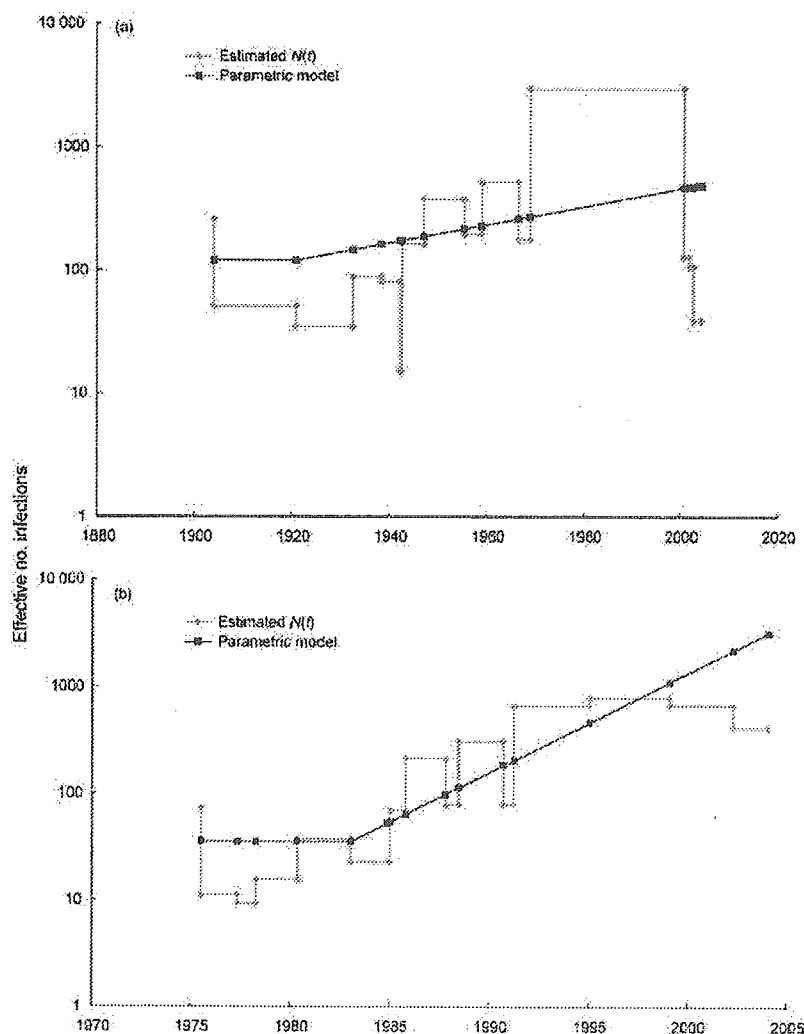


Fig. 3. ML estimates of $N(t)$ on the effective number of (a) HEV genotype 3 and (b) HEV genotype 4 infections in Japan. The parametric model is indicated by the grey line and stepwise plots by the black line, which represent corresponding non-parametric estimates of $N(t)$ (number as a function of time). Genetic distances have been transformed into a time scale of years by using estimates of the molecular clock in the partial RNA polymerase region of HEV.

(2003). The estimated k_s values from HAV strains isolated from a clam-associated outbreak varied from 0.038 for VP0 to 0.29 for VP1. Similarly, we estimated the evolutionary rate of HEV by using Japan-indigenous genotype 3 and genotype 4 strains isolated over time. The rate was estimated to be approximately 0.8×10^{-3} nucleotide substitutions per site year⁻¹ by two independent methods, which was around half of our previously estimated rate (Takahashi *et al.*, 2004b). One of the reasons is that the molecular-evolutionary rate would depend on estimated genes; the previous report (Takahashi *et al.*, 2004b) used complete sequences, whereas this study used only RNA polymerase sequences. Another reason is that the previous extrapolation of substitution rate on pairwise (direct) comparisons can give overestimates of the molecular clock and hence divergent times of HEV species, as reported previously (Ina *et al.*, 1994). Based on the molecular clock, we traced the demographic history of HEV in Japan and the indigenization time was suggested to be similar (approx. 1900), but the spread time was quite different, between HEV genotypes 3 and 4 (1920s versus 1980s). Interestingly, in addition, the evolutionary growth of genotype 3 has been quite slow since the 1920s, whereas genotype 4 strains have spread rapidly in Sapporo since the 1980s.

Zoonosis has been implicated in HEV transmission. The first animal strain of HEV to be isolated and characterized was a swine HEV from a pig in the USA in 1997 (Meng *et al.*, 1997). Since then, many swine HEV strains, which exhibit extensive genetic heterogeneity, have been identified worldwide and shown to be genetically related closely to strains of human HEV (Chandler *et al.*, 1999; Hsieh *et al.*, 1999; Huang *et al.*, 2002; Okamoto *et al.*, 2001; Wang *et al.*, 2002). Recent findings suggested an interspecies HEV transmission between boar and deer in their wild life (Takahashi *et al.*, 2004a) and that both animals might serve as an infection source for human beings. More recently, wild mongoose was newly added to the list of HEV-reservoir animals in Japan (Nakamura *et al.*, 2006). Notwithstanding the importance of these wild animals, pigs for food must be the major reservoirs of HEV: a recent Japanese study indicated that anti-HEV antibodies were detected in 1448 (58 %) of 2500 pigs from 2 to 6 months of age at 25 commercial swine farms in Japan (Takahashi *et al.*, 2003). The importance of transmission of HEV from pigs to humans was further supported by a recent field study in Indonesia: Muslim people, for whom it is a taboo to eat or contact pigs, were significantly less frequently positive for anti-HEV than Hindu people (2.0 vs 20 %) (Surya *et al.*, 2005).

Our molecular-evolutionary analyses suggested that HEV entered Japan around 1900. If we have traced the origin of Japan-indigenous HEV correctly back to about 100 years ago, what happened at that time in relevance to HEV's indigenization? Several kinds of Yorkshire pig were imported for the first time in the history of Japan from the UK in 1900, by the Japanese government's policy to introduce excellent domestic animals for food in Western

countries to Japan, as a measure to nutritionally strengthen the people (especially soldiers) of this formerly vegetarian country. Since then, the Yorkshire pigs have been propagated in Japan and, in the 1930s, thousands of pigs were reported all over Japan (<http://okayama.lin.go.jp/history/2-3-1-2.htm>), suggesting that the domestic spread of HEV might have been associated with the popularization of pigs for food in Japan. Indeed, a previous phylogenetic analysis of a 304 bp nucleotide sequence (ORF2) obtained from the two UK swine strains showed a close relationship with Japanese swine strains in genotype 3 (Banks *et al.*, 2004), indicating that Japanese genotype 3 may have been imported from the UK. On the other hand, Japanese genotype 4 strains were related phylogenetically to Asian strains in Taiwan and China. As the HEV found in wild boars living in the Iriomote Island, near Taiwan, was of genotype 4 (unpublished results), the source of Japanese genotype 4 might be from Taiwan or the mainland of China. Note that a phylogenetic analysis showed that the Japanese swine and human HEV strains segregated into four clusters [three genotype 3 clusters (one major Japanese and two minor clusters) and one genotype 4 cluster], with the highest nucleotide identity being 94.4–100 % between swine and human strains in each cluster (Takahashi *et al.*, 2003), suggesting that swine have served as one of the most important reservoirs for HEV to be transmitted to humans. The possible risk factor for transmission of HEV was to have eaten uncooked or undercooked pig liver and/or intestine 1–2 months before the onset of hepatitis E in Hokkaido, Japan (Mizuo *et al.*, 2005). Such eating habits, which are particularly unique to those living in Hokkaido (Sapporo is one of the big cities there) in recent decades, might be one of the reasons that HEV has been widespread in this area since 1990, as supported by our molecular-evolutionary analyses in this study.

In conclusion, based on our present data, the indigenization and domestic spread of HEV in Japan are proposed to have been associated with the importation and popularization of pigs for food in Japan. However, there still remains a possibility of different scenarios. Another animal(s) might have carried the virus to Japan: for example, mongoose was imported from India to Japan in 1910 (Nakamura *et al.*, 2006).

Acknowledgements

Contributions of authors are as follows: Y. T. performed molecular-clock analyses and wrote the manuscript; K. T. amplified and sequenced viral isolates; E. O. helped Y. T. with the molecular-clock analyses; J.-H. K., K. S., A. M., A. H., H. M., H. S., Y. A. and T. K. provided HEV RNA-positive sera to K. T. for sequence determinations; M. M. supervised the molecular-clock analyses; and S. M. designed the study and helped Y. T. to write the manuscript. This work was supported in part by grants from the Ministry of Health, Labour and Welfare of Japan (200400676A) and from the United States–Japan Collaborative Medical Science Program (Hepatitis Panel). We greatly appreciate Dr Oliver G. Pybus (Department of Zoology, University of Oxford, Oxford, UK) for his enlightening advice on molecular-evolutionary analyses using GENIE v3.5.

References

- Banks, M., Bendall, R., Grierson, S., Heath, G., Mitchell, J. & Dalton, H. (2004). Human and porcine hepatitis E virus strains, United Kingdom. *Emerg Infect Dis* 10, 953–955.
- Chandler, J. D., Riddell, M. A., Li, F., Love, R. J. & Anderson, D. A. (1999). Serological evidence for swine hepatitis E virus infection in Australian pig herds. *Vet Microbiol* 68, 95–105.
- Harrison, T. J. (1999). Hepatitis E virus – an update. *Liver* 19, 171–176.
- Hasegawa, M., Kishino, H. & Yano, T. (1985). Dating of the human–ape splitting by a molecular clock of mitochondrial DNA. *J Mol Evol* 22, 160–174.
- Hsieh, S.-Y., Meng, X.-J., Wu, Y.-H., Liu, S.-T., Tam, A. W., Lin, D.-Y. & Liaw, Y.-F. (1999). Identity of a novel swine hepatitis E virus in Taiwan forming a monophyletic group with Taiwan isolates of human hepatitis E virus. *J Clin Microbiol* 37, 3828–3834.
- Huang, F. F., Haqshenas, G., Guenette, D. K., Halbur, P. G., Schommer, S. K., Pierson, F. W., Toth, T. E. & Meng, X. J. (2002). Detection by reverse transcription-PCR and genetic characterization of field isolates of swine hepatitis E virus from pigs in different geographic regions of the United States. *J Clin Microbiol* 40, 1326–1332.
- Ina, Y., Mizokami, M., Ohba, K. & Gojobori, T. (1994). Reduction of synonymous substitutions in the core protein gene of hepatitis C virus. *J Mol Evol* 38, 50–56.
- Kabrane-Lazizi, Y., Fine, J. B., Elm, J. & 7 other authors (1999). Evidence for widespread infection of wild rats with hepatitis E virus in the United States. *Am J Trop Med Hyg* 61, 331–335.
- Lemey, P., Pybus, O. G., Wang, B., Saksena, N. K., Salemi, M. & Vandamme, A.-M. (2003). Tracing the origin and history of the HIV-2 epidemic. *Proc Natl Acad Sci U S A* 100, 6588–6592.
- Matsuda, H., Okada, K., Takahashi, K. & Mishiroy, S. (2003). Severe hepatitis E virus infection after ingestion of uncooked liver from a wild boar. *J Infect Dis* 188, 944.
- Meng, X.-J., Purcell, R. H., Halbur, P. G., Lehman, J. R., Webb, D. M., Tsareva, T. S., Haynes, J. S., Thacker, B. J. & Emerson, S. U. (1997). A novel virus in swine is closely related to the human hepatitis E virus. *Proc Natl Acad Sci U S A* 94, 9860–9865.
- Meng, X.-J., Halbur, P. G., Shapiro, M. S., Govindarajan, S., Bruna, J. D., Mushahwar, I. K., Purcell, R. H. & Emerson, S. U. (1998). Genetic and experimental evidence for cross-species infection by swine hepatitis E virus. *J Virol* 72, 9714–9721.
- Meng, X. J., Wiseman, B., Elvinger, F., Guenette, D. K., Toth, T. E., Engle, R. E., Emerson, S. U. & Purcell, R. H. (2002). Prevalence of antibodies to hepatitis E virus in veterinarians working with swine and in normal blood donors in the United States and other countries. *J Clin Microbiol* 40, 117–122.
- Mizuo, H., Yazaki, Y., Sugawara, K., Tsuda, F., Takahashi, M., Nishizawa, T. & Okamoto, H. (2005). Possible risk factors for the transmission of hepatitis E virus and for the severe form of hepatitis E acquired locally in Hokkaido, Japan. *J Med Virol* 76, 341–349.
- Nakamura, M., Takahashi, K., Taira, K., Taira, M., Ohno, A., Sakugawa, H., Arai, M. & Mishiroy, S. (2006). Hepatitis E virus infection in wild mongooses of Okinawa, Japan: demonstration of anti-HEV antibodies and a full-genome nucleotide sequence. *Hepatol Res* (in press).
- Nishizawa, T., Takahashi, M., Mizuo, H., Miyajima, H., Gotanda, Y. & Okamoto, H. (2003). Characterization of Japanese swine and human hepatitis E virus isolates of genotype IV with 99% identity over the entire genome. *J Gen Virol* 84, 1245–1251.
- Okamoto, H., Takahashi, M., Nishizawa, T., Fukai, K., Muramatsu, U. & Yoshikawa, A. (2001). Analysis of the complete genome of indigenous swine hepatitis E virus isolated in Japan. *Biochem Biophys Res Commun* 289, 929–936.
- Purcell, R. H. & Emerson, S. U. (2001). Hepatitis E virus. In *Fields Virology*, 4th edn, pp. 3051–3061. Edited by D. M. Knipe, P. M. Howley, D. E. Griffin, R. A. Lamb, M. A. Martin, B. Roizman & S. E. Straus. Philadelphia, PA: Lippincott Williams & Wilkins.
- Pybus, O. G. & Rambaut, A. (2002). GENIE: estimating demographic history from molecular phylogenies. *Bioinformatics* 18, 1404–1405.
- Pybus, O. G., Charleston, M. A., Gupta, S., Rambaut, A., Holmes, E. C. & Harvey, P. H. (2001). The epidemic behavior of the hepatitis C virus. *Science* 292, 2323–2325.
- Pybus, O. G., Drummond, A. J., Nakano, T., Robertson, B. H. & Rambaut, A. (2003). The epidemiology and iatrogenic transmission of hepatitis C virus in Egypt: a Bayesian coalescent approach. *Mol Biol Evol* 20, 381–387.
- Rambaut, A. (2000). Estimating the rate of molecular evolution: incorporating non-contemporaneous sequences into maximum likelihood phylogenies. *Bioinformatics* 16, 395–399.
- Sánchez, G., Bosch, A. & Pintó, R. M. (2003). Genome variability and capsid structural constraints of hepatitis A virus. *J Virol* 77, 452–459.
- Surya, I. G. P., Kornia, K., Suwardewa, T. G. A., Mulyanto Tsuda, F. & Mishiroy, S. (2005). Serological markers of hepatitis B, C, and E viruses and human immunodeficiency virus type-1 infections in pregnant women in Bali, Indonesia. *J Med Virol* 75, 499–503.
- Takahashi, M., Nishizawa, T., Miyajima, H., Gotanda, Y., Iita, T., Tsuda, F. & Okamoto, H. (2003). Swine hepatitis E virus strains in Japan form four phylogenetic clusters comparable with those of Japanese isolates of human hepatitis E virus. *J Gen Virol* 84, 851–862.
- Takahashi, K., Kitajima, N., Abe, N. & Mishiroy, S. (2004a). Complete or near-complete nucleotide sequences of hepatitis E virus genome recovered from a wild boar, a deer, and four patients who ate the deer. *Virology* 330, 501–505.
- Takahashi, K., Toyota, J., Karino, Y., Kang, J.-H., Maekubo, H., Abe, N. & Mishiroy, S. (2004b). Estimation of the mutation rate of hepatitis E virus based on a set of closely related 7.5-year-apart isolates from Sapporo, Japan. *Hepatol Res* 29, 212–215.
- Tamada, Y., Yano, K., Yatsushashi, H., Inoue, O., Mawatari, F. & Ishibashi, H. (2004). Consumption of wild boar linked to cases of hepatitis E. *J Hepatol* 40, 869–870.
- Tanaka, Y., Hanada, K., Mizokami, M., Yeo, A. E. T., Shih, J. W.-K., Gojobori, T. & Alter, H. J. (2002). A comparison of the molecular clock of hepatitis C virus in the United States and Japan predicts that hepatocellular carcinoma incidence in the United States will increase over the next two decades. *Proc Natl Acad Sci U S A* 99, 15584–15589.
- Tanaka, Y., Hanada, K., Orito, E. & 8 other authors (2005). Molecular evolutionary analyses implicate injection treatment for schistosomiasis in the initial hepatitis C epidemics in Japan. *J Hepatol* 42, 47–53.
- Tei, S., Kitajima, N., Takahashi, K. & Mishiroy, S. (2003). Zoonotic transmission of hepatitis E virus from deer to human beings. *Lancet* 362, 371–373.
- Wang, Y.-C., Zhang, H.-Y., Xia, N.-S. & 11 other authors (2002). Prevalence, isolation, and partial sequence analysis of hepatitis E virus from domestic animals in China. *J Med Virol* 67, 516–521.
- Yazaki, Y., Mizuo, H., Takahashi, M., Nishizawa, T., Sasaki, N., Gotanda, Y. & Okamoto, H. (2003). Sporadic acute or fulminant hepatitis E in Hokkaido, Japan, may be food-borne, as suggested by the presence of hepatitis E virus in pig liver as food. *J Gen Virol* 84, 2351–2357.

特集II 本邦におけるE型肝炎の実態

E型肝炎ウイルスの進化
速度と本邦における拡散
時期の推定*田中靖人**
高橋和明***
三代俊治***
溝上雅史****Key Words** : hepatitis E virus, molecular clock, genotype, spread time

はじめに

E型肝炎ウイルス(HEV)は急性E型肝炎をひき起こす病原体であり, 流行性にE型肝炎が発生しているアジア, アフリカおよび中米などの発展途上国に常在している. 先進諸国でも散発性のHEV感染は稀ながら報告されていたが, それらは流行国からの帰国後発症する「輸入感染症」とみなされていた. しかし, 1990年代後半に入り, 欧米から旅行歴のない非A非B非C型急性肝炎例の中にHEVが原因と思われる症例が報告され, さらに流行地とは異なるgenotypeがE型肝炎発症に関わることが明らかとなった. わが国においても, 2001年に海外渡航歴のない原因不明の急性肝炎症例から国内型HEV株が分離され報告されたことが端緒となり, 国内型E型肝炎の報告が相次いだ^{1)~4)}. しかし実際, HEVがいつ頃から本邦に存在していたかは不明である.

HEVはきわめて多様性に富むウイルスであり, ヒト・ブタ・イノシシ・シカなどの哺乳類から得られたHEVはすべて同一種と考えられており^{5)~9)}, 現在までにgenotype I~IVまでに分類されている¹⁰⁾. 本邦では主にgenotype IIIとIVが存在す

る⁴⁾¹¹⁾. ここでは, こうしたウイルス変異を基にしてHEVの進化速度(変異速度)を求め, 本邦におけるHEV拡散時期を分子進化学的手法を用いて推定した.

進化速度(変異速度)

C型肝炎ウイルス(HCV)は同一個体内に持続感染することから, 同一個体内でのウイルス変異からその変異速度を推定することは容易であった¹²⁾¹³⁾. HEVは一過性感染であるため, 同一個体内での検討は不可能であるが, ある地域の中では, 個体から個体への一過性性感染を繰り返しながら持続感染している. したがって, 同一地域から取られた複数のHEV株は, 系統樹において有意なクラスターを形成する場合があります, これらの塩基配列を基にして変異速度を求めることは可能である.

われわれはこれまでに少なくとも2つのクラスターを見出している(図1). 全塩基配列が報告されている日本株13本を使用した系統解析の結果, 北海道より分離された4本の株がgenotype IVの中でもっとも有意なクラスターを形成した. これらの株は1995年3月28日に分離されたJSM-Sap95, 2000年11月10日に分離されたJKK-Sap00, 2002年8月30日に分離されたJYW-Sap02, 2002年9月14日に分離されたJTS-Sap02である¹⁴⁾. こ

* Tracing HEV endemic in Japan.

** Yasuhito TANAKA, M.D., Ph.D. & Masashi MIZOKAMI, M.D., Ph.D.: 名古屋市立大学大学院医学研究科臨床分子情報医学講座(〒467-8601 名古屋市瑞穂区瑞穂町川澄1); Department of Clinical Molecular Informative Medicine, Nagoya City University Graduate School of Medical Sciences, Nagoya 467-8601, JAPAN

*** Kazuaki TAKAHASHI, M.D. & Shunji MISHIRO, M.D.: 東芝病院研究部

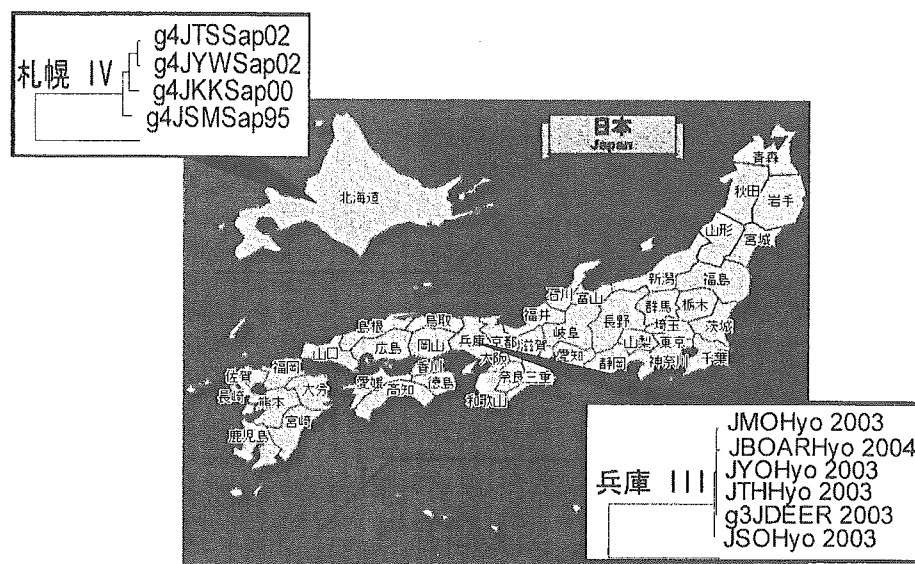


図1 札幌および兵庫のクラスター

これらの株を用いて系統樹を作成し、これらの推定先祖配列からの遺伝子距離(枝の長さ)を縦軸に、採取年月日を横軸に取り、linear regression解析によりHEVの進化速度をその傾きとして求めると、約 4.8×10^{-4} /site/year, さらに同義置換数から計算すると 1.8×10^{-3} /site/yearと推定された(図2-a). もう一つのクラスターは、兵庫で2003年にシカ刺摂取後に集団E型肝炎が発生した事例から得られたHEV 5株および翌年に近隣地域のイノシシから得られたHEV株である⁹⁾. 同様にlinear regression解析により、HEVの進化速度は、同義置換数から計算すると 2.1×10^{-3} /site/yearと推定された(図2-b). 面白いことに、これらの進化速度はHCV遺伝子配列から推定されている数字に非常に近似していた.

本邦におけるHEVの分岐時期

前述のように、本邦におけるHEVはgenotype IIIとIVが主体である. では、いつごろからこれらの株は本邦に存在したのであろうか? この疑問に答えるためには、できるだけ正確なウイルス進化速度の推定がもっとも重要となる. 先に述べた全塩基配列での検討でHEVの進化速度は、同義置換で $(1.8-2.1) \times 10^{-3}$ /site/yearと推定されたが、分岐時期(HEVが本邦に持ち込まれた時期)を推定するには全塩基配列の報告が少ないため

正確な値を求めることは困難である. Preliminaryな解析結果を図3に示すが、genotype III, IVともに1900年前後にはすでに本邦に存在していたと思われる.

HEV拡散時期の推定:

Effective population sizeを用いて

このようにHEV全長での解析は報告例が少ないためこれ以上の解析は困難であるが、より短い領域であれば塩基配列の新規決定も容易であり、多数のHEV株を用いたより正確な解析が可能となる. HEVは、全長約7,200ntの一本鎖プラス鎖RNAウイルスであり、3つのopen reading frame(ORF)からなる. ORF1がコードするpolyproteinの中には、HCV同様RNA helicaseやRNA-dependent RNA polymeraseが含まれ、HEVにとって必要不可欠な重要な部位である. こうした機能的に重要な部位は、従来よりウイルス進化速度を検討するには適した領域と考えられており¹²⁾, われわれはGDD motifを含むRNA polymerase領域(821nt)のHEV株の塩基配列を新たに決定し、分子進化学的に進化速度および拡散時期を再検討した. 系統解析の結果(図4), 外国株とは明らかに異なる日本固有のクラスターがgenotype III (24例)およびgenotype IV (25例)に存在し、これらの配列に基づいて以下の検討を行った.

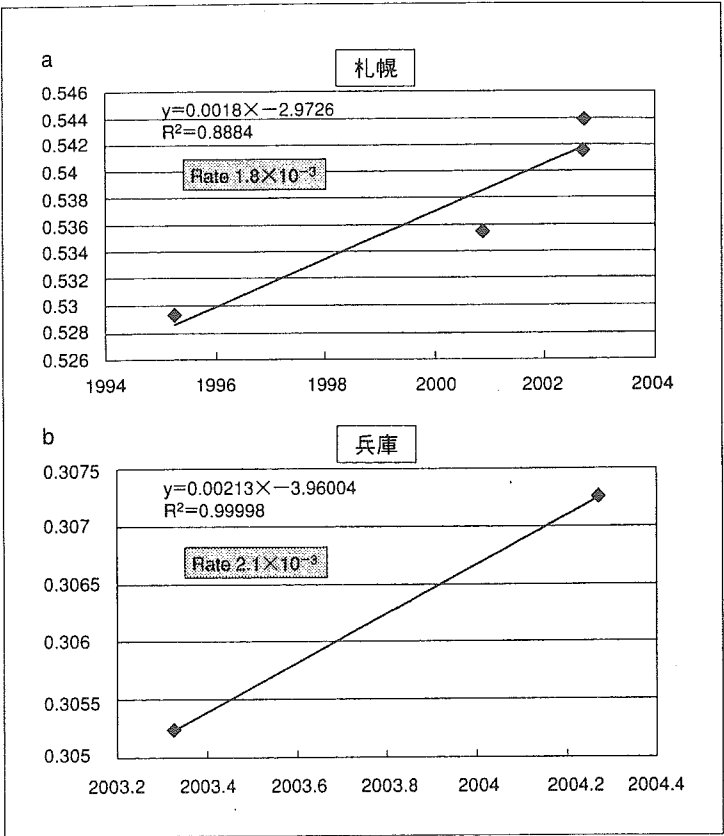


図 2 同義置換数に基づいた進化速度(変異速度)

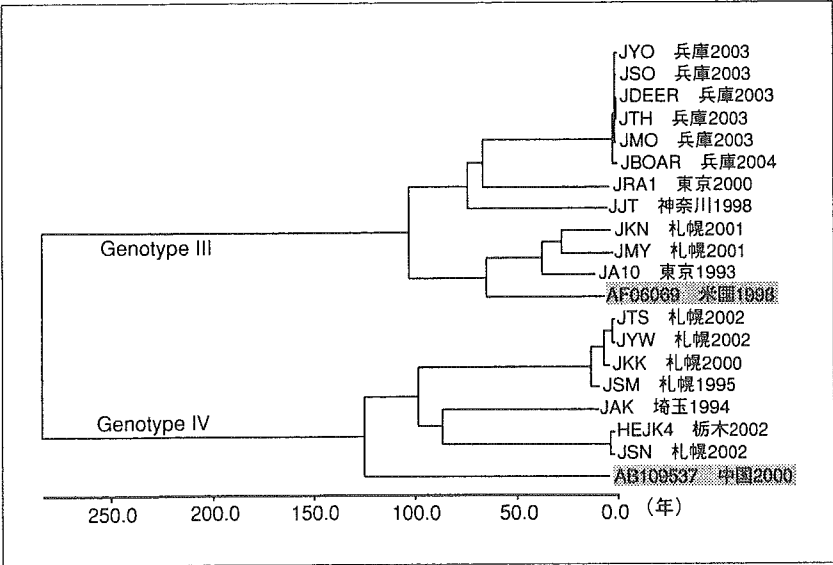


図 3 全塩基配列に基づく系統樹
下段に推定分岐時期(年)を示す。

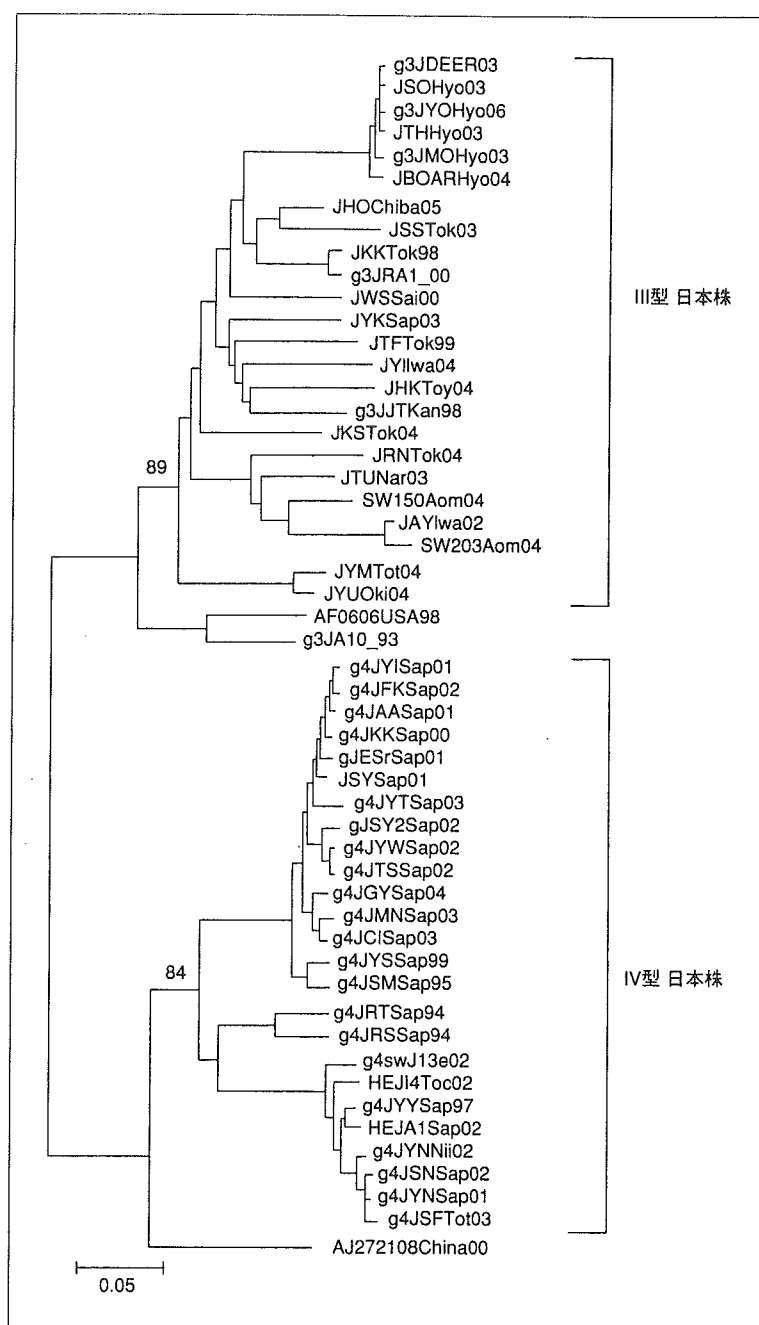


図4 GDD motifを含むRNA polymerase領域(821nt)の系統樹
Ⅲ,Ⅳ型ともに日本固有のクラスターを形成する。末尾は採取年を示す。

1. 進化速度の検証
2. 分岐時期の推定
3. 拡散時期の推定

これまでにわれわれは、集団遺伝学によく用いられているcoalescent theory(effective popula-

tion sizeの解析)をウイルス進化に応用し、日米におけるHCV拡散時期の違いを推定している¹⁵⁾。このeffective population sizeという概念はそもそも集団遺伝学の概念であり、集団の有効な大きさと略される。ここでは、簡略化して説明した

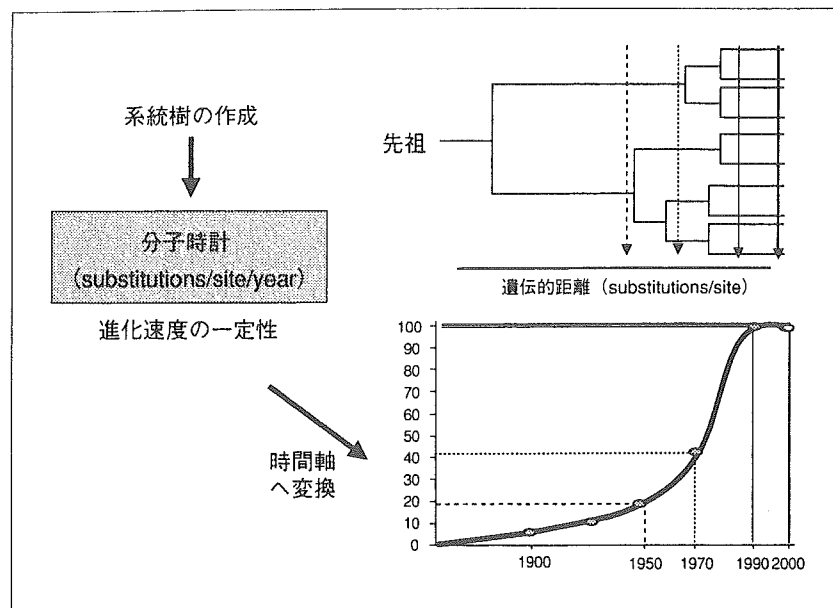


図5 相対的 HEV population(推定感染数)の推定方法

い。図5に示すように現在のHEV遺伝子配列を基にして、たとえば2000年におけるHEV population数(推定感染数)を100%と仮定すると、過去に遡るにしたがいpopulation数は減少していくことになる。この手法を用いると、HEVが過去から現在にかけて、いつごろから増加してきたかが推定可能となり、このeffective population sizeの解析からHEV genotype IIIとIVの分岐時期(HEVが本邦に入った時期)を推定すると、両タイプともに約100年前に遡ることがわかった。その後の推移は両タイプで大きく異なり、genotype IIIは1920年ごろより緩やかに増加しているのに対し、genotype IVは、最近10~20年の間に北海道を中心に増加していることがわかった。

本邦における社会的背景

前述しているようにHEV感染は人畜共通感染症として、ブタからヒトへの感染がクローズアップされている。直接証拠こそないが、ブタからヒトへのHEV感染を示唆するデータはこれまでに複数報告されている^{16)~18)}。とくに、北海道札幌市と北見市において、ブタの肝臓が感染源であったという報告は特記すべきものである⁷⁾。

そこで本邦におけるブタに関する歴史を紐解いてみると、明治政府はわが国の富国強兵策の一環

として、西洋のすぐれた家畜を国内ですみやかに増殖普及する目的で、明治33年(1900年)に広島県七塚原に種牛牧場を設置して、イギリスから大ヨークシャー種、中ヨークシャー種、小ヨークシャー種、パークシャー種を輸入して、ここに繁殖し、優良種豚の生産配布事業を行っていた。大正(1912年)から昭和初期にわたるブタの飼養は、4~5年を周期として増減を繰り返しながらも漸増を続け、昭和13年(1938年)には、戦前における最高の8,900頭を記録していた(<http://okayama.lin.go.jp/history/2-3-1-2.htm>)。こうした本邦における1900年以降のブタの普及とHEV感染の拡散が関与している可能性が示唆された。

一方、北海道ではどうであったのか? 1990年頃までの北海道では圧倒的にジンギスカン(=羊肉)が主流であったようだが、なぜかその頃からブタを主体とした焼肉やホルモンが大衆化して、ジンギスカンに取って代わっている(三代先生談)。とくに前述の北見市は、日本一のホルモンの町と言われており、こうしたブタ(ブタレバーなど)摂取の増加が近年北海道でIV型が増えた要因の一つかもしれない。さらなる疫学調査が必要である。

おわりに

現在のウイルス株の塩基(遺伝子)配列を基に

して過去のHEVの歴史を推定することが可能となった。すでにHCVでも複数報告しているように、こうした分子進化学的解析は分子疫学的検討に有用性が高く、あらゆるウイルス進化の解析に応用可能と思われた。

文 献

- 1) Takahashi K, Iwata K, Watanabe N, et al. Full-genome nucleotide sequence of a hepatitis E virus strain that may be indigenous to Japan. *Virology* 2001 ; 287 : 9-12.
- 2) Takahashi K, Kang JH, Ohnishi S, et al. Genetic heterogeneity of hepatitis E virus recovered from Japanese patients with acute sporadic hepatitis. *J Infect Dis* 2002 ; 185 : 1342-5.
- 3) Tei S, Kitajima N, Takahashi K, et al. Zoonotic transmission of hepatitis E virus from deer to human beings. *Lancet* 2003 ; 362 : 371-3.
- 4) Mizuo H, Suzuki K, Takikawa Y, et al. Polyphyletic strains of hepatitis E virus are responsible for sporadic cases of acute hepatitis in Japan. *J Clin Microbiol* 2002 ; 40 : 3209-18.
- 5) Okamoto H, Takahashi M, Nishizawa T, et al. Analysis of the complete genome of indigenous swine hepatitis E virus isolated in Japan. *Biochem Biophys Res Commun* 2001 ; 289 : 929-36.
- 6) Takahashi M, Nishizawa T, Miyajima H, et al. Swine hepatitis E virus strains in Japan form four phylogenetic clusters comparable with those of Japanese isolates of human hepatitis E virus. *J Gen Virol* 2003 ; 84 : 851-62.
- 7) Yazaki Y, Mizuo H, Takahashi M, et al. Sporadic acute or fulminant hepatitis E in Hokkaido, Japan, may be food-borne, as suggested by the presence of hepatitis E virus in pig liver as food. *J Gen Virol* 2003 ; 84 : 2351-7.
- 8) Tei S, Kitajima N, Ohara S, et al. Consumption of uncooked deer meat as a risk factor for hepatitis E virus infection : an age- and sex-matched case-control study. *J Med Virol* 2004 ; 74 : 67-70.
- 9) Takahashi K, Kitajima N, Abe N, et al. Complete or near-complete nucleotide sequences of hepatitis E virus genome recovered from a wild boar, a deer, and four patients who ate the deer. *Virology* 2004 ; 330 : 501-5.
- 10) Schlauder GG, Mushahwar IK. Genetic heterogeneity of hepatitis E virus. *J Med Virol* 2001 ; 65 : 282-92.
- 11) Takahashi K, Kang JH, Ohnishi S, et al. Full-length sequences of six hepatitis E virus isolates of genotypes III and IV from patients with sporadic acute or fulminant hepatitis in Japan. *Intervirology* 2003 ; 46 : 308-18.
- 12) Ina Y, Mizokami M, Ohba K, et al. Reduction of synonymous substitutions in the core protein gene of hepatitis C virus. *J Mol Evol* 1994 ; 38 : 50-6.
- 13) Tanaka H, Yoshino H, Kobayashi E, et al. Molecular investigation of hepatitis E virus infection in domestic and miniature pigs used for medical experiments. *Xenotransplantation* 2004 ; 11 : 503-10.
- 14) Takahashi K, Toyota J, Karino Y, et al. Estimation of the mutation rate of hepatitis E virus based on a set of closely related 7.5-year-apart isolates from Sapporo, Japan. *Hepatol Res* 2004 ; 29 : 212-5.
- 15) Tanaka Y, Hanada K, Mizokami M, et al. Inaugural Article : A comparison of the molecular clock of hepatitis C virus in the United States and Japan predicts that hepatocellular carcinoma incidence in the United States will increase over the next two decades. *Proc Natl Acad Sci USA* 2002 ; 99 : 15584-9.
- 16) Hsieh SY, Meng XJ, Wu YH, et al. Identity of a novel swine hepatitis E virus in Taiwan forming a monophyletic group with Taiwan isolates of human hepatitis E virus. *J Clin Microbiol* 1999 ; 37 : 3828-34.
- 17) Withers MR, Correa MT, Morrow M, et al. Antibody levels to hepatitis E virus in North Carolina swine workers, non-swine workers, swine, and murids. *Am J Trop Med Hyg* 2002 ; 66 : 384-8.
- 18) Wibawa ID, Muljono DH, Mulyanto, et al. Prevalence of antibodies to hepatitis E virus among apparently healthy humans and pigs in Bali, Indonesia : Identification of a pig infected with a genotype 4 hepatitis E virus. *J Med Virol* 2004 ; 73 : 38-44.

Essential Elements of the Capsid Protein for Self-Assembly into Empty Virus-Like Particles of Hepatitis E Virus

Tian-Cheng Li,^{1*} Naokazu Takeda,¹ Tatsuo Miyamura,¹ Yoshiharu Matsuura,² Joseph C. Y. Wang,³ Helena Engvall,³ Lena Hammar,³ Li Xing,³ and R. Holland Cheng^{3,4}

Department of Virology II, National Institute of Infectious Diseases, Gakuen 4-7-1, Musashi-Murayama, Tokyo 208-0011,¹ and Department of Molecular Virology, Research Institute for Microbial Diseases, Osaka University, Suita-shi, Osaka 565-0871,² Japan; Karolinska Institute, Department of Biosciences, 141 57 Huddinge, Sweden³; and Department of Molecular and Cellular Biology, University of California, Davis, California 95616⁴

Received 21 April 2005/Accepted 20 July 2005

Hepatitis E virus (HEV) is a noncultivable virus that causes acute liver failure in humans. The virus's major capsid protein is encoded by an open reading frame 2 (ORF2) gene. When the recombinant protein consisting of amino acid (aa) residues 112 to 660 of ORF2 is expressed with a recombinant baculovirus, the protein self-assembles into virus-like particles (VLPs) (T.-C. Li, Y. Yamakawa, K. Suzuki, M. Tatsumi, M. A. Razak, T. Uchida, N. Takeda, and T. Miyamura, *J. Virol.* 71:7207–7213, 1997). VLPs can be found in the culture medium of infected Tn5 cells but not in that of Sf9 cells, and the major VLPs have lost the C-terminal 52 aa. To investigate the protein requirement for HEV VLP formation, we prepared 14 baculovirus recombinants to express the capsid proteins truncated at the N terminus, the C terminus, or both. The capsid protein consisting of aa residues 112 to 608 formed VLPs in Sf9 cells, suggesting that particle formation is dependent on the modification process of the ORF2 protein. In the present study, electron cryomicroscopy and image processing of VLPs produced in Sf9 and Tn5 cells indicated that they possess the same configurations and structures. Empty VLPs were found in both Tn5 and Sf9 cells infected with the recombinant containing an N-terminal truncation up to aa residue 125 and C-terminal to aa residue 601, demonstrating that the aa residues 126 to 601 are the essential elements required for the initiation of VLP assembly. The recombinant HEV VLPs are potential mucosal vaccine carrier vehicles for the presentation of foreign antigenic epitopes and may also serve as vectors for the delivery of genes to mucosal tissue for DNA vaccination and gene therapy. The results of the present study provide useful information for constructing recombinant HEV VLPs having novel functions.

Hepatitis E virus (HEV), which causes severe acute liver failure, belongs to the genus *Hepevirus* in the family *Hepeviridae* (22). HEV contains an approximately 7.2-kb single-stranded positive-sense RNA molecule (21). The RNA is 3' polyadenylated and includes three open reading frames (ORF). ORF1, mapped in the 5' half of the genome, encodes viral nonstructural proteins (7, 12). ORF2, located at the 3' terminus of the genome, encodes a protein-forming viral capsid (11, 25). ORF3, mapped between ORF1 and ORF2, encodes a 13.5-kDa protein that is associated with the membrane as well as with the cytoskeleton fraction (27). This protein is shown to be phosphorylated by the cellular mitogen-activated protein kinase (6, 8). The ORF3 protein may have a regulatory function (6, 8). Ever since HEV was first discovered in 1980 and visualized by immune electron microscopy in 1983 (2), many efforts have been made, using different expression systems, to express the structural protein (5, 11, 17, 26). It is particularly important to characterize the viral protein because so far no practical cell culture system for growing HEV is available. Only one neutralization epitope has been identified; it maps between amino acids 578 and 607 of the ORF2 protein (pORF2) (18).

The expression of foreign proteins in baculovirus systems opens the prospect of studying HEV capsid assembly, since virus-like particles (VLPs) of pronounced spikes on the surface can be formed with the recombinant protein expressed with this system (11, 25). This VLP is capable of inducing systemic and mucosal immune responses in experimental animals (9). With an oral inoculation of 10 mg of recombinant HEV VLPs, cynomolgus monkeys can develop anti-HEV immunoglobulin M (IgM), IgG, and IgA responses and protect against HEV infection (10). All these data suggest that VLPs are a candidate HEV vaccine.

The VLPs produced from Tn5 cells appear as T=1 icosahedral particles, which are composed of 60 copies of truncated pORF2 (25). The protein contains two distinctive domains: the shell (S) domain forms the semiclosed icosahedral shell, while the protrusion (P) domain interacts with the neighboring proteins to form the protrusion. The projection of T=1 recombinant HEV VLPs appears as spikes decorated with spherical rings (25), which fits with the morphology obtained from negatively stained HEV native virions. The diameter of these VLPs, 27 nm, is less than that reported for partially purified native virions (16). However, VLPs retain the antigenicity of the native HEV virion by designated antigenic sites at the P domain and by the capsid connection at the S domain. The particles appear empty, with no significant RNA-like density inside. The N-terminal region of pORF2 is rich in positively charged amino acid residues and may interact with RNA mol-

* Corresponding author. Mailing address: Department of Virology II, National Institute of Infectious Diseases, Gakuen 4-7-1, Musashi-Murayama, Tokyo 208-0011, Japan. Phone: (81)-42-561-0771. Fax: (81)-42-561-4729. E-mail: litc@nih.go.jp.

TABLE 1. Oligonucleotides used in the construction of baculovirus recombinants

Recombinant baculovirus	Forward primer ^a	Reverse primer ^b
Ac[n111]	AAGGATCC ATG GCGGTCGCTCCAGCCCATGACACCCGCCAGT	GGTCTAGACTATAACTCCCGAGTTTACCACCTTCTACTT
Ac[n111c52]	AAGGATCC ATG GCGGTCGCTCCAGCCCATGACACCCGCCAGT	AATCTAGACTATGCTAGCGCAGAGTGGGGGGCTAAAA
Ac[n111c58]	AAGGATCC ATG GCGGTCGCTCCAGCCCATGACACCCGCCAGT	AATCTAGACTAGGCTAAACAGCAACCCGAGAGATGG
Ac[n111c59]	AAGGATCC ATG GCGGTCGCTCCAGCCCATGACACCCGCCAGT	AATCTAGACTATAAAACAGCAACCCGAGAGATGGAGA
Ac[n111c60]	AAGGATCC ATG GCGGTCGCTCCAGCCCATGACACCCGCCAGT	AATCTAGACTAAACAGCAACCCGAGAGATGGAGACGG
Ac[n111c64]	AAGGATCC ATG GCGGTCGCTCCAGCCCATGACACCCGCCAGT	AATCTAGACTAAGAGATGGAGACGGGACCAGCACCCA
Ac[n111c72]	AAGGATCC ATG GCGGTCGCTCCAGCCCATGACACCCGCCAGT	AATCTAGACTAACCAGGCTAGTGGTGTAAGTGAAAA
Ac[c52]	CAGGATCC ATG GCGGTCGCTCCAGCCCATGACACCCGCCAGT	AATCTAGACTATGCTAGCGCAGAGTGGGGGGCTAAAA
Ac[n123]	AAGGATCC ATG GACTGTCGACTCTCGCGCGCCATCTT	GGTCTAGACTATAACTCCCGAGTTTACCACCTTCTACTT
Ac[n124]	AAGGATCC ATG GTCGACTCTCGCGCGCCATCTT	GGTCTAGACTATAACTCCCGAGTTTACCACCTTCTACTT
Ac[n125]	AAGGATCC ATG GACTCTCGCGCGCCATCTTTCGG	GGTCTAGACTATAACTCCCGAGTTTACCACCTTCTACTT
Ac[n126]	AAGGATCC ATG TCTCGCGCGCCATCTTTCGGCGG	GGTCTAGACTATAACTCCCGAGTTTACCACCTTCTACTT
Ac[n130]	CAGGATCC ATG ATCTTTCGGCGCGCAGTATAATCTATC	GGTCTAGACTATAACTCCCGAGTTTACCACCTTCTACTT
Ac[n125c59]	AAGGATCC ATG GACTCTCGCGCGCCATCTTTCGG	AATCTAGACTATAAAACAGCAACCCGAGAGATGGAGA

^a BamHI (underlined) and an initiation codon (bold) are indicated.
^b XbaI (underlined) and a stop codon (bold) are indicated.

ecules (21). Thus, the deletion of the N-terminal 111 amino acid (aa) residues and the insufficient volume of the central cavity may lead to the failure of RNA encapsidation (25). Cell type dependence in the VLP formation of the recombinant capsid protein was observed when aa residues 112 to 660 of ORF2 were expressed with a recombinant baculovirus in two insect cell lines, Tn5 and Sf9. In Tn5 cells, two major bands, having molecular masses of 58 kDa (58K) and 53 kDa (53K), were found in the cell lysate, while a peptide in the VLPs comprising a 53K protein was found in the culture medium. The 53K protein has been designated as either the 50K or 54K protein in previous studies (9, 11). In Sf9 cells, an additional peptide with a size between that of 58K and that of 53K was found in the cell lysate. However, no VLP was recovered from the culture medium. In Tn5 cells, terminal sequencing revealed that 58K and 53K proteins have the same first 15 aa in the N terminus and that a posttranslation cleavage by cellular protease(s) occurred at the pORF2 C termini and converted 58K into 53K. An independent but similar observation was obtained when pORF2 of the Pakistani strain was expressed in Sf9 cells (17) where several immunoreactive proteins were detected in the cell lysate, and a 53K protein was secreted into the culture medium, but no VLP was found. Further investigation of pORF2 expression in Sf9 and Tn5 cells may allow us to understand the mechanism underlying the subunit assembly and particle formation of the recombinant HEV capsid. We analyzed particle formation with pORF2 containing a series of truncated deletions at the N- and/or C-terminal region. In both Sf9 and Tn5 cells, amino acid residues 126 to 601 appeared to form the pORF2 core structure and were capable of self-assembling into VLPs. These results indicated that the cell dependence on particle formation is due to the difference between Sf9 and Tn5 cells in the modification process of pORF2.

MATERIALS AND METHODS

Generation of recombinant baculoviruses and expression of capsid proteins. DNA fragments encoding the N- and/or C-terminal aa-truncated pORF2 were amplified by PCR using plasmid pHEV5134/7161 as a template. Plasmid pHEV5134/7161 containing a full-length genotype 1 (G1) HEV pORF2 was

described previously (11). The primers used in the construction of baculovirus recombinants are shown in Table 1. Amplified DNA fragments were purified by using a QIAGEN PCR purification kit (QIAGEN, Valencia, CA), digested with restriction enzymes, and ligated with baculovirus transfer vector pVL1393 (Pharmingen, San Diego, CA). An insect cell line derived from *Spodoptera frugiperda* (Sf9) (19) (Riken Cell Bank, Tsukuba, Japan) was cotransfected with a linearized wild-type *Autographa californica* nuclear polyhedrosis virus DNA (Pharmingen), and the transfer vectors were cotransfected by the Lipofectin-mediated method as specified by the manufacturer (Gibco BRL, Gaithersburg, MD). The cells were incubated at 26.5°C in TC-100 medium (Gibco BRL) supplemented with 8% fetal bovine serum and 0.26% Bacto tryptose phosphate broth (Difco Laboratories, Detroit, MI). The proteins in the culture medium and cell lysate were separated by sodium dodecyl sulfate-polyacrylamide gel electrophoresis (SDS-PAGE) and analyzed by Western blot assay using serum from a patient with acute hepatitis E (11). Each recombinant virus was plaque purified three times. The baculovirus recombinants thus obtained were designated as Ac[n111], Ac[n111c52], Ac[n111c58], Ac[n111c59], Ac[n111c60], Ac[n111c64], Ac[n111c72], Ac[c52], Ac[n123], Ac[n124], Ac[n125], Ac[n126], Ac[n130], and Ac[n125c59]; a schematic diagram is shown in Fig. 1. Both insect Sf9 and Tn5 cells, the latter from a *Trichoplusia ni* insect cell line, BTI-Tn-5B1-4 (Invitrogen, San Diego, CA), were infected with recombinant baculoviruses at a multiplicity of infection of 10 and incubated for 5 days at 26.5°C as previously described (11, 23). **Purification of VLPs.** The culture medium was harvested on day 5 after infection. The intact cells, cell debris, and progeny baculoviruses were removed by centrifugation at 10,000 × g for 90 min. The supernatant was then spun at 25,000 rpm for 2 h in a Beckman SW28 rotor. The resulting pellet was resuspended in 4.5 ml EX-CELL 405 at 4°C overnight. After mixing with 1.96 g of CsCl, the sample was centrifuged at 35,000 rpm for 24 h at 4°C in a Beckman SW50.1 rotor. The visible white band (at a density of 1.285 g/ml) was harvested by puncturing the tubes with a 21-gauge needle, diluted with EX-CELL 405 medium, and then centrifuged again in a Beckman TLA45 rotor at 45,000 rpm (125,000 × g) for 2 h to remove CsCl. The VLPs were placed on a carbon-coated grid, and the proteins were allowed to be absorbed into the grid for 5 min. After being rinsed with distilled water, the sample was stained with a 1% aqueous uranyl acetate solution and examined with a Hitachi H-7000 electron microscope operating at 75 kV. **Terminal amino acid sequence analysis.** The VLPs were further purified by 5 to ~30% sucrose gradient centrifugation at 35,000 rpm for 2 h in a Beckman SW50.1 rotor. The visible white band was harvested as described above, diluted with EX-CELL 405, and again centrifuged at 45,000 rpm for 2 h in a Beckman TLA55 rotor to precipitate the VLPs. N-terminal aa microsequencing was carried out using 100 pmol of the protein by Edman automated degradation on an Applied Biosystems model 477 protein sequencer, and C-terminal aa sequencing was performed by Applied Biosystems. **SDS-PAGE and Western blot analysis.** Dispersed insect cells were incubated for 20 min at room temperature to allow the cells to attach to culture flasks in TC-100 (Sf9 cells) or EX-CELL 405 (Tn5 cells) medium. The culture medium was removed, and the cells were infected with the recombinant baculoviruses at

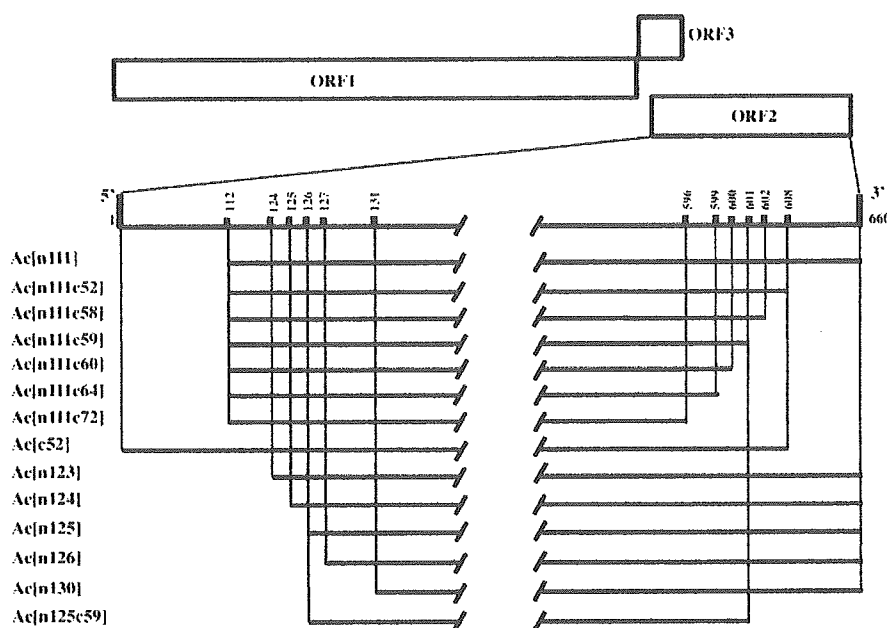


FIG. 1. Genome organization of HEV and schematic diagram of recombinant baculovirus vectors. DNA fragments encoding N- and C-terminal aa-truncated ORF2 were prepared by PCR with the primers listed in Table 1 and were used to construct 14 recombinant baculoviruses. Full-length pORF2 consisted of 660 aa. The N- and C-terminal aa numbers of the truncated protein are indicated.

a multiplicity of infection of 10. Virus adsorption was carried out for 1 h at room temperature, and then the cells were incubated at 26.5°C. The proteins in the cell lysate and in the culture medium were separated by 10% SDS-PAGE and stained with Coomassie blue. For Western blotting, the proteins in the SDS-PAGE gel were electrophoretically transferred onto a nitrocellulose membrane. The membrane was then blocked with 5% skim milk in 50 mM Tris-HCl (pH 7.4)–150 mM NaCl and reacted with a patient's serum from an acute phase. Human IgG antibody was detected by using alkaline phosphatase-conjugated goat anti-human immunoglobulin (1:1,000 dilution) (DAKO A/S, Copenhagen, Denmark). Nitroblue tetrazolium chloride and 5-bromo-4-chloro-3-indolyl phosphate P-toluidine were used as coloring agents (Bio-Rad Laboratories).

Cryo-electron microscopy (cryo-EM) and image reconstruction. A 3- μ l drop of purified HEV VLP (~1 mg/ml) was applied onto holey carbon film. After extra solution was wiped away with filter paper, the grid was rapidly plunged into liquid ethane surrounded by liquid nitrogen. Thus embedded in a thin layer of vitrified ice, the specimen was then transferred via a Gatan 626 cryo-transfer system to a Philips CM120 microscope. The specimen was observed at liquid nitrogen temperature and photographed at a magnification of 45,000. Each area was photographed twice, with defocus levels of 1 μ m and 3 μ m, respectively. The electron dose of each exposure was less than 10 electrons/ \AA^2 . The selected electron micrographs were digitized with a Zeiss scanner at a step size of 14 μ m, corresponding to 3.1 \AA at the specimen. The images were reconstructed according to icosahedral symmetry with Fourier-Basel procedures (4, 28). Briefly, the particle orientation and center of each image were estimated with the EMPFT program, where the structure of Tn5-produced HEV VLP was used as the initial model (1). The first reconstruction was generated from selected images and used as a model to refine the orientation and center parameters. After itinerant runs of EMPFT, the parameters were stable and appeared unchanged from one EMPFT run to another. The final reconstruction was computed by combining 353 images at a resolution of 23 \AA . The surface-rendering map was generated with the NAG Explorer program combined with custom-created modules.

Mass spectrometry. The mass spectrometry experiment was done with a Reflex III mass spectrometer from Bruker, equipped with gridless delayed extraction. The samples were mixed with an equal volume of a saturated solution of sinapinic acid (Sigma Chemical Co., St. Louis, MO) in 33% (vol/vol) acetonitrile and 0.1% (vol/vol) trifluoroacetic acid. On the target plate, a thin layer was prepared with a saturated solution of sinapinic acid in ethanol. A sample volume of 0.5 μ l was applied to a thin layer of sinapinic acid and allowed to crystallize. Data were acquired in the linear instrument mode. Data were processed and evaluated by XMASS software from Bruker.

RESULTS

C-terminal 52-amino-acid deletion is necessary for formation of VLPs in Sf9 cells. To understand the mechanism underlying VLP formation in Sf9 and Tn5 cells, we prepared a series of baculovirus recombinants expressing pORF2 with different deletions at the N- and/or C-terminal region (Table 1 and Fig. 1). The cell lysate and culture medium of infected insect cells were analyzed by Western blotting. In a previous study, the N-terminal 111 aa-truncated HEV pORF2 was expressed by a recombinant baculovirus, Ac[n111], in both insect cells (11). Two major proteins, ~58K and ~53K, were detected in both cell lysates. The 53K protein was released into cell culture medium and assembled into VLPs in Tn5 cells but not in Sf9 cells (11).

Analysis of the N- and C-terminal aa sequences of the VLPs revealed that the N terminus was at aa residue 112 and the C terminus ended at aa residue 608, indicating that the C-terminal 52 aa of ORF2 were deleted. The protein that forms VLPs contains 497 amino acids (112 to ~608), and its molecular mass was about 53K. An N-terminal 111 aa- and C-terminal 52 aa-truncated construct, Ac[n111c52], was generated, and the protein was expressed in both Sf9 and Tn5 cells. As expected, a single 53K protein was found in both Sf9 and Tn5 cell lysates (Fig. 2, Ac[n111c52] lanes in Sf9 and Tn5). Interestingly, these 53K proteins were released into both culture media as VLPs, as observed by electron microscopy (Fig. 3). The particle appeared empty and homogenous in size. Therefore, C-terminal truncation to aa residue 608 is crucial for particle formation and release into Sf9 cells.

Ac[n111c58] and Ac[n111c59] encode truncated pORF2s with an N-terminal 111-aa deletion and respective C-terminal deletions of 58 and 59 aa. The expressed proteins migrated to

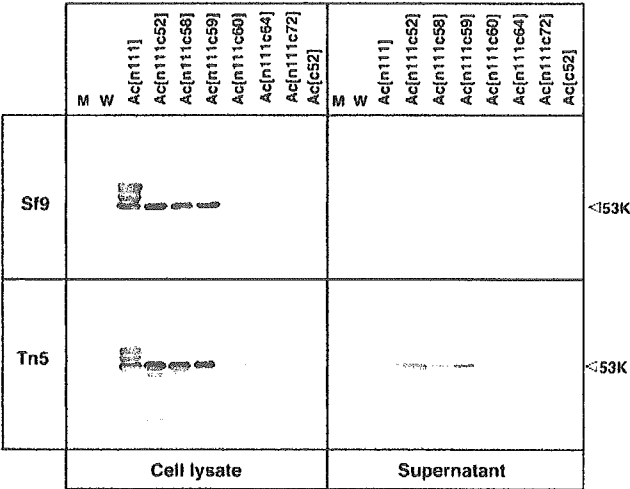


FIG. 2. Western blot assay of truncated pORF2 expressed in Sf9 and Tn5 cells. Eight recombinant baculoviruses, Ac[n111], Ac[n111c52], Ac[n111c58], Ac[n111c59], Ac[n111c60], Ac[n111c64], Ac[n111c72], and Ac[c52], were used to infect the insect cells. Ten microliters of the culture medium (right column) and 5 μ l of the cell lysate (left column) were separated by 10% SDS-PAGE, and HEV-specific proteins were detected by Western blot analysis using the serum of a patient with acute hepatitis E. M, molecular weight markers; W, wild-type baculovirus-infected cells.

a position similar to that of 53K and appeared in both cell lysates as well as in the culture medium (Fig. 2); both were also assembled into VLPs (data not shown). In contrast, truncated pORF2 from Ac[n111c60], Ac[n111c64], and Ac[n111c72] was not released into the culture medium to detectable levels, and VLP was not formed even though protein expression remained similar to those of the other constructs (Fig. 2). Instead, a

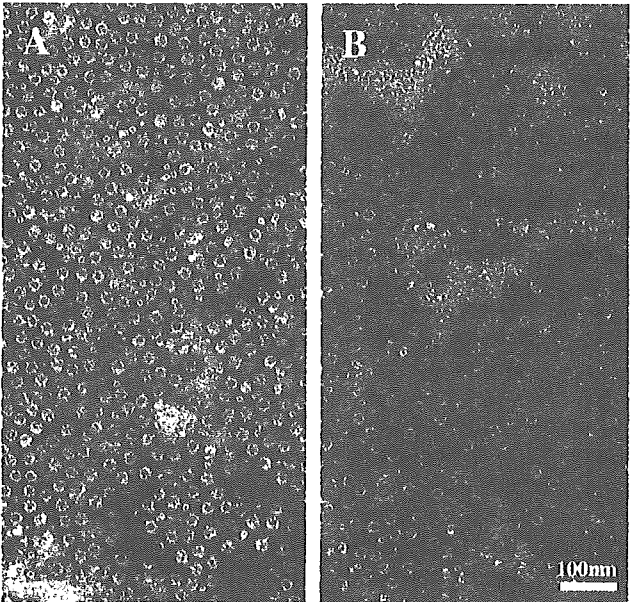


FIG. 3. EM of the HEV VLPs generated in Tn5 (A) and Sf9 (B) cells with recombinant baculovirus Ac[n111c52]. The VLPs were stained with 2% uranyl acetate. Bar, 100 nm.

protein with a molecular mass of 42 kDa was detected in both of the cell lysates as well as in the culture medium by Western blot analysis. When pORF2 with a C-terminal 52-aa deletion was expressed with a recombinant baculovirus, Ac[c52], two major proteins, 65K and \sim 53K, were observed in infected Tn5 and Sf9 cell lysates 5 days postinfection (p.i.). However, these two proteins were not detected in their culture media (Fig. 2, Ac[c52] lanes in Sf9 and Tn5). These results indicated that aa residues before 601 were essential to the formation of VLPs.

VLPs produced in Sf9 and Tn5 cells possess the same configurations and structures. The morphology of the VLPs generated in Sf9 cells appeared to be similar to that generated in Tn5 cells, as observed in the negatively stained particles (Fig. 3). To investigate the structural properties of these two released VLPs, we performed cryo-electron microscopy and image processing using VLPs produced in Tn5 cells. The electron cryomicrographs showed that the particle projected as a spiky hollow sphere, indicating that no RNA-like density was packed inside the capsid (Fig. 4A). The image processing was done according to the icosahedral procedure. The rotational symmetry of 522 was applied to reconstruct the final three-dimensional structure. The reconstructed VLP displayed a T=1 surface lattice with protruding density located at each of 30 twofold axes (Fig. 4B). The VLP was composed of 60 copies of pORF2, and the protruding density consisted of dimeric, projecting domains from twofold-related peptides. The particle diameter was 270 \AA , measured from the three-dimensional reconstruction. The protein shell was 85 \AA thick at the twofold axes. A channel can be observed under each protruding density. The protruding density was about 43 \AA high, and the twofold platform was 56 \AA in the long axes (data not shown). The threefold-related dimers formed a regular triangle, and the dimer-dimer distance was 76 \AA measured from center to center (Fig. 4B). Molecular interactions at the icosahedral threefold region appeared much stronger than those at the fivefold region. There was no significant difference in radial density distribution between Tn5- and Sf9-produced VLPs (Fig. 4C).

We further determined the composition of the particles obtained from Sf9 and Tn5 cells using mass spectrometry (Fig. 5). HEV VLPs produced from Tn5 and Sf9 cells with recombinant baculovirus Ac[n111c52] were analyzed. In both cases, the major density peak was monitored at the position corresponding to a mass of 53 kDa. The peak was symmetrically distributed, and a shoulder tip can be found in both cases. The shoulder tip was about 1 kDa larger than the main density peak. The signals further confirmed that the molecular mass of truncated pORF2 was 53 kDa, disregarding the production cell lines.

Essential N-terminal amino acids for VLP formation. Deletion of the N-terminal 111 residues is necessary for particle formation, which is consistent with our previous observation (11). The subsequent question is how many amino acids can be removed from pORF2 N termini without changing its capability to form VLPs. We made five constructs to express proteins with 123-, 124-, 125-, 126-, and 130-aa deletions at the N terminus by using five recombinant baculoviruses: Ac[n123], Ac[n124], Ac[n125], Ac[n126], and Ac[n130], respectively. As shown in Fig. 6, three proteins, having molecular masses of 58 to 51 kDa, were detected by Western blotting in both cell lysates at 5 days p.i., and the largest bands (58 to \sim 57K) were

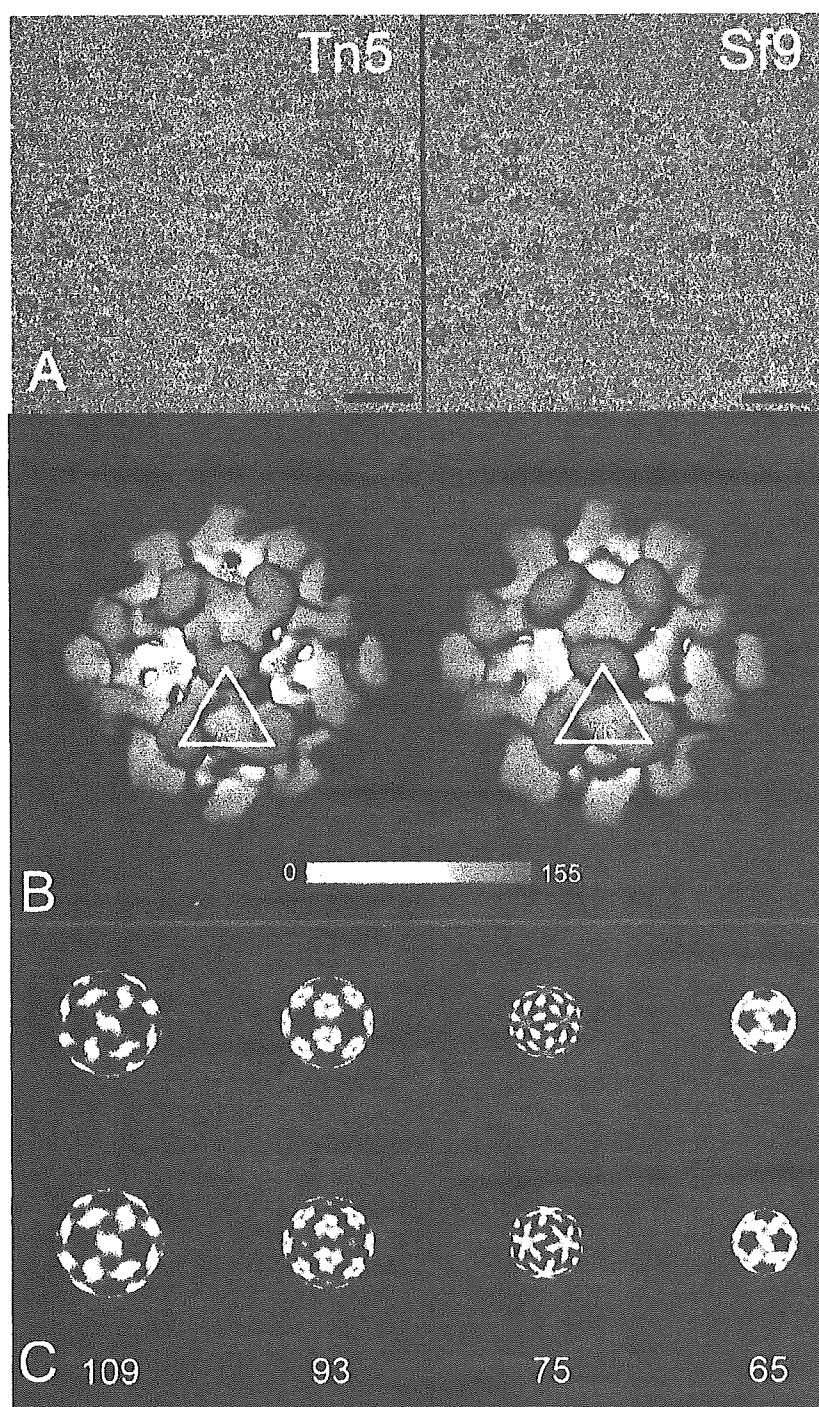


FIG. 4. HEV VLP structures determined by cryo-electron microscopy and image reconstruction. (A) Cryo-electron micrograph of ice-embedded HEV VLPs produced from Tn5 and Sf9 cells. The bar corresponds to 100 nm. (B) Surface-shaded representation of HEV VLP structures viewed along icosahedral twofold axes. VLPs from both Tn5 (left panel) and Sf9 (right panel) cells were color coded according to the radius, as indicated in the scale bar. The adjacent protruding spikes remain at equal distances of 76 Å (white lines). The asterisks mark the positions of three adjacent icosahedral fivefold axes. (C) Sequential radial density projections generated from the twofold-oriented density map at corresponding radii. The protein density appears as the light color, while the background density is black.

thought to be the primary translation products encoded by N-terminal 123, 124, 125, 126, and 130 aa-truncated ORF2. In Tn5 cells, a C-terminal 52-aa-deleted product, about 51K protein, was the major protein to be efficiently released into the

culture medium, where VLP formation occurred in Ac[n123]-, Ac[n124]-, and Ac[n125]-infected Tn5 cells (data not shown). Although the 51K protein was released into the culture medium, no VLP formation occurred in Ac[n126]- or Ac[n130]-

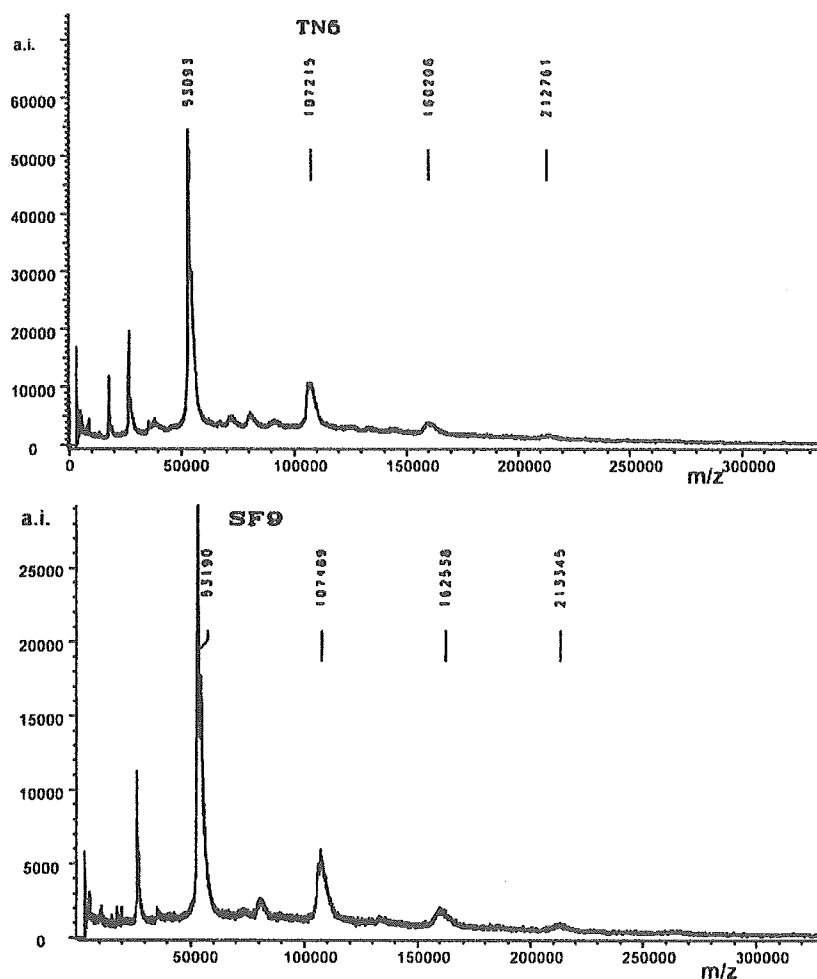


FIG. 5. Mass spectra from purified HEV VLPs displayed as the counts of isotope abundance (a.i.) versus mass/charge values (m/z). HEV VLPs produced from Tn5 (top panel) and Sf9 (bottom panel) cells with recombinant baculovirus Ac[n111c52] gave consistent mass spectra in which the abundant elements show similar m/z values at 53,000, 107,000, and 160,000.

infected Tn5 cells. In contrast, the 51K protein was not released into the culture medium in infected Sf9 cells (Fig. 6). These results demonstrated that aa residues after 125 were essential to the formation of VLPs.

When Ac[n125c59], an N-terminal 125 aa- and C-terminal 59 aa-truncated recombinant baculovirus, was expressed in Sf9 and Tn5 cells, the 51K protein was detected in both cell lysates and the culture media, where VLP formation occurred in both insect cell types (Fig. 6). This confirmed our observation that a C-terminal deletion of 52 to 59 amino acids was required for particle formation when Sf9 cells were used.

DISCUSSION

HEV is enigmatic due to the virus's inability to grow in conventional cell culture. Large quantities of the HEV capsid protein carrying antigenicity and immunogenicity comparable to those of the native virion have been generated for a long time, because the capsid protein is a key molecule for the diagnosis of hepatitis E as well as for vaccine development.

We previously found that when an N-terminal 111 aa-trun-

cated ORF2 protein was expressed in Tn5 and Sf9 cells, two major peptides, having molecular masses of 58 and 53 kDa, were generated in both cells, and only the 53-kDa protein generated in Tn5 cells was released into culture medium and self-assembled into VLPs (11). The 58K protein presented the primary translation product, and the 53K protein is a processing product from the 58K protein. In this study, we examined the difference between Tn5 and Sf9 cells in HEV ORF2 gene expression and found that when a recombinant baculovirus (Ac[n111c52]) harboring a construct of the C-terminal 52-aa deletion was used, no difference between Sf9 and Tn5 cells in protein translation and particle formation was found. The observation that Ac[n111] failed to produce VLPs in Sf9 cells raised a question about the posttranslation modification in insect cells. In Tn5 cells, the levels of protein expression by Ac[n111] and Ac[n111c52] appeared to be similar. Therefore, it is likely that the 58K protein was incorrectly processed in Sf9 cells, thus affecting VLP assembly.

In addition, when Sf9 insect cells were infected with Ac[n111], the expressed proteins were localized in the cyto-

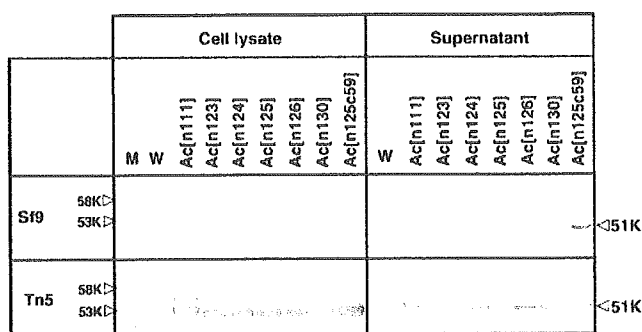


FIG. 6. Expression of N-terminally truncated pORF2 in Sf9 and Tn5 cells infected with Ac[n123], Ac[n124], Ac[n125], Ac[n126], Ac[n130], and Ac[n125c59]. A Western blot assay was carried out as described in the legend to Fig. 2. Ac[n111] was included for the expression of the 58K and 53K proteins. M, molecular weight markers; W, wild-type baculovirus-infected cells.

plasm and observed as inclusion-like bodies (one to four structures per cell) by EM (25). In contrast, when Sf9 cells were infected with Ac[n111c52], there were no inclusion-like bodies (data not shown), and the expressed proteins were localized evenly in the cytoplasm. Concomitantly, expressed protein was poorly detected in the culture medium from Ac[n111]-infected Sf9 cells at 3 days p.i., whereas a large amount of the 53K protein was detected in the culture medium from Ac[n111c52]-infected Sf9 cells. These findings suggest that the C-terminal aa of ORF2 might affect the localization, and subsequently the release, of the capsid protein from the insect cells. However, we do not yet know whether the VLPs form before release in infected cells or after release in culture medium.

The presence of Leu601 in pORF2 is important for the formation of HEV VLPs. A protein with a longer (580 to 610) deletion of aa residues was aberrant in protein folding; this may reduce the ORF2 homo-oligomerization (24). The prediction of the secondary structure based on protein sequence suggests two β -strand motifs in the region between aa 580 and 601 (580 to ~589 and 593 to ~601). The failure in the particle assembly with Ac[n111c60] is due to incomplete formation of this β -strand motif. Although aa 111 to 601 and aa 111 to 602 formed VLPs, the yield of each of these was about 10 to 20% of the yields of aa 111 to 660 (data not shown). This is in contrast to the fact that the levels of protein expression inside the cells were similar in these constructs. This observation further confirmed that stability of the C-terminal β -strand motif is essential for VLP assembly.

The N-terminal 111-aa-deletion was found to be essential for cellular membrane dissociation of pORF2 expressed in insect cells (17, 24). We extended the N-terminal deletion up to Val125 without altering the ability to form HEV VLPs (Fig. 6). The ORF2 protein exhibits two-domain folding (25), with a domain organization similar to those of the norovirus (NV) capsid protein (15) and the tomato bushy stunt virus capsid protein (14). The N-terminal aa residues 112 to 125 may be the arm region extending from the S domain into the particle interior. In NV, the N-terminal region appeared to serve as a switch controlling the S domain configuration in the assembly process (3). Removal of the first 20 amino acids did not affect NV-like particle self-assembly, but a longer deletion at the

N-terminal region did (3). Thus, residues 112 to 125 are putatively located in the HEV virion interior and may regulate VLP assembly.

Tn5 and Sf9 are insect cell lines that are commonly used in recombinant protein expression. The Tn5 cell is becoming more and more popular because it yields higher quantities of tissue factor than Sf9. Under optimum conditions, Tn5 cells produce 28-fold more secreted soluble tissue factor than Sf9 cells on a per-cell basis (23). In this paper, we report the difference between Tn5 and Sf9 cells in a protein synthesis system. The ORF2 protein underwent posttranslational cleavage, which is crucial for HEV VLP assembly. Although the HEV virion assembly mechanism remains unclear, our data indicate that the region consisting of ORF2 residues 126 to 601 is the kernel element for the monomer-monomer interaction and thus initiates VLP assembly.

Recombinant HEV VLPs themselves can be candidates for parenteral as well as oral hepatitis E vaccines (9, 10), and these VLPs have potential as mucosal vaccine carrier vehicles for the presentation of foreign antigenic epitopes through oral administration (13). Furthermore, HEV VLPs can be a vector for gene delivery to mucosal tissue for the purposes of DNA vaccination and gene therapy (20). The results of the present study provide the basic tool to construct VLPs having novel functions.

ACKNOWLEDGMENTS

We thank Tomoko Mizoguchi for secretarial work, Thomas Kieselbach for help with the mass spectrometry, and Leif Bergman for building EXPLORER modules.

The study was supported in part by Health and Labor Sciences Research Grants, including Research on Emerging and Re-emerging Infectious Diseases, Research on Hepatitis, Research on Human Genome, Tissue Engineering, and Research on Food Safety, from the Ministry of Health, Labor and Welfare, Japan. This work was sponsored by grants from the Swedish Research Council to R.H.C. and L.X. A grant from the National Science Council, Taiwan, supported the work of J.C.Y.W.

REFERENCES

- Baker, T. S., and R. H. Cheng. 1996. A model-based approach for determining orientations of biological macromolecules imaged by cryoelectron microscopy. *J. Struct. Biol.* 116:120–130.
- Balayan, M. S., A. G. Andjaparidze, S. S. Savinskaya, E. S. Ketiladze, D. M. Braginsky, A. P. Savinov, and V. F. Poleschuk. 1983. Evidence for a virus in non-A, non-B hepatitis transmitted via the fecal-oral route. *Intervirology* 20:23–31.
- Bertolotti-Ciarlet, A., L. J. White, R. Chen, B. V. Prasad, and M. K. Estes. 2002. Structural requirements for the assembly of Norwalk virus-like particles. *J. Virol.* 76:4044–4055.
- Cheng, R. H. 2000. Visualization on the grid of virus-host interactions, p. 141–153. In L. Johnsson (ed.), *Simulation and visualization on the grid*. Springer-Verlag, New York, N.Y.
- He, J., A. W. Tam, P. O. Yarbough, G. R. Reyes, M. Carl, P. O. Yarbough, A. W. Tam, K. E. Fry, K. Krawczynski, K. A. McCaustland, D. W. Bradley, and G. R. Reyes. 1993. Expression and diagnostic utility of hepatitis E virus putative structural proteins expressed in insect cells. *J. Clin. Microbiol.* 31:2167–2173.
- Kar-Roy, A., H. Korkaya, R. Oberoi, S. K. Lal, and S. Jameel. 2004. The hepatitis E virus open reading frame 3 protein activates ERK through binding and inhibition of the MAPK phosphatase. *J. Biol. Chem.* 279:28345–28357.
- Koonin, E. V., A. E. Gorbalenya, M. A. Purdy, M. N. Rozanov, G. R. Reyes, and D. W. Bradley. 1992. Computer-assisted assignment of functional domains in the nonstructural polyprotein of hepatitis E virus: delineation of an additional group of positive-strand RNA plant and animal viruses. *Proc. Natl. Acad. Sci. USA* 89:8259–8263.
- Korkaya, H., S. Jameel, D. Gupta, S. Tyagi, R. Kumar, M. Zafrullah, M. Mazumdar, S. K. Lal, L. Xiaofang, D. Sehgal, S. R. Das, and D. Sahai. 2001.

- The ORF3 protein of hepatitis E virus binds to Src homology 3 domains and activates MAPK. *J. Biol. Chem.* **276**:42389–42400.
9. Li, T. C., N. Takeda, and T. Miyamura. 2001. Oral administration of hepatitis E virus-like particles induces a systemic and mucosal immune response in mice. *Vaccine* **19**:3476–3484.
 10. Li, T. C., Y. Suzuki, Y. Ami, T. N. Dhole, T. Miyamura, and N. Takeda. 2004. Protection of cynomolgus monkeys against HEV infection by oral administration of recombinant hepatitis E virus-like particles. *Vaccine* **22**:370–377.
 11. Li, T. C., Y. Yamakawa, K. Suzuki, M. Tatsumi, M. A. Ruzak, T. Uchida, N. Takeda, and T. Miyamura. 1997. Expression and self-assembly of empty virus-like particles of hepatitis E virus. *J. Virol.* **71**:7207–7213.
 12. Magden, J., N. Takeda, T. C. Li, P. Auvinen, T. Ahola, T. Miyamura, A. Merits, and L. Kaariainen. 2001. Virus-specific mRNA capping enzyme encoded by hepatitis E virus. *J. Virol.* **75**:6249–6255.
 13. Niikura, M., S. Takamura, G. Kim, S. Kawai, M. Saijo, S. Morikawa, I. Kurane, T. C. Li, N. Takeda, and Y. Yasutomi. 2002. Chimeric recombinant hepatitis E virus-like particles as an oral vaccine vehicle presenting foreign epitopes. *Virology* **293**:273–280.
 14. Olson, A. J., G. Bricogne, and S. C. Harrison. 1983. Structure of tomato bush stunt virus. IV. The virus particle at 2.9 Å resolution. *J. Mol. Biol.* **171**:61–93.
 15. Prasad, B. V., M. E. Hardy, T. Dokland, J. Bella, M. G. Rossmann, and M. K. Estes. 1999. X-ray crystallographic structure of the Norwalk virus capsid. *Science* **286**:287–290.
 16. Purcell, R. H., and S. U. Emerson. 2001. Hepatitis E virus, p. 3051–3061. In D. M. Knipe and P. M. Howley (ed.), *Fields virology*, 4th ed., vol. 1. Lippincott Williams & Wilkins, Philadelphia, Pa.
 17. Robinson, R. A., W. H. Burgess, S. U. Emerson, R. S. Leibowitz, S. A. Sosnovtseva, S. Tsarev, and R. H. Purcell. 1998. Structural characterization of recombinant hepatitis E virus ORF2 proteins in baculovirus-infected insect cells. *Protein Expr. Purif.* **12**:75–84.
 18. Schofield, D. J., J. Glamann, S. U. Emerson, and R. H. Purcell. 2000. Identification by phage display and characterization of two neutralizing chimpanzee monoclonal antibodies to the hepatitis E virus capsid protein. *J. Virol.* **74**:5548–5555.
 19. Stewart, L. M. D., and R. D. Possee. 1993. Baculovirus expression vectors, p. 227–256. In A. J. Davidson and R. M. Elliotts (ed.), *Molecular virology: a practical approach*. IRL Press, Oxford, United Kingdom.
 20. Takamura, S., M. Niikura, T. C. Li, N. Takeda, S. Kusagawa, Y. Takebe, T. Miyamura, and Y. Yasutomi. 2004. DNA vaccine-encapsulated virus-like particles derived from an orally transmissible virus stimulate mucosal and systemic immune responses by oral administration. *Gene Ther.* **11**:628–635.
 21. Tam, A. W., M. M. Smith, M. E. Guerra, C. C. Huang, D. W. Bradley, K. E. Fry, and G. R. Reyes. 1991. Hepatitis E virus (HEV): molecular cloning and sequencing of the full-length viral genome. *Virology* **185**:120–131.
 22. *Virus Taxonomy*. 2002. <http://www.ictvdb.iacr.ac.uk/ictv/fr-frst-g.htm>.
 23. Wickham, T. J., and G. R. Nemerow. 1993. Optimization of growth methods and recombinant protein production in BT1-Tn-5B1-4 insect cells using the baculovirus expression system. *Biotechnol. Prog.* **9**:25–30.
 24. Xiaofang, L., M. Zafrullah, F. Ahmad, and S. Jameel. 2001. A C-terminal hydrophobic region is required for homo-oligomerization of the hepatitis E virus capsid (ORF2) protein. *J. Biomed. Biotechnol.* **1**:122–128.
 25. Xing, L., K. Kato, T. Li, N. Takeda, T. Miyamura, L. Hammar, and R. H. Cheng. 1999. Recombinant hepatitis E capsid protein self-assembles into a dual-domain T = 1 particle presenting native virus epitopes. *Virology* **265**:35–45.
 26. Yarbough, P. O., A. W. Tam, K. E. Fry, K. Krawczynski, K. A. McCaustland, D. W. Bradley, and G. R. Reyes. 1991. Hepatitis E virus: identification of type-common epitopes. *J. Virol.* **65**:5790–5797.
 27. Zafrullah, M., M. H. Ozdener, S. K. Panda, and S. Jameel. 1997. The ORF3 protein of hepatitis E virus is a phosphoprotein that associates with the cytoskeleton. *J. Virol.* **71**:9045–9053.
 28. Zhong, Y., J. Cheng, Y. Liu, J. Dong, J. Yang, and L. Zhang. 2000. Expression of human single-chain variable fragment antibody against non-structural protein 3 of hepatitis C virus antigen in *e. coli*. *Zhonghua Gan Zang Bing Zhi* **8**:171–173. (In Chinese.)

Simultaneous Detection of Immunoglobulin A (IgA) and IgM Antibodies against Hepatitis E Virus (HEV) Is Highly Specific for Diagnosis of Acute HEV Infection

Masaharu Takahashi,¹ Shigeyuki Kusakai,² Hitoshi Mizuo,³ Kazuyuki Suzuki,⁴
Kuniko Fujimura,⁵ Kazuo Masuko,⁶ Yoshiki Sugai,⁷ Tatsuya Aikawa,⁸
Tsutomu Nishizawa,¹ and Hiroaki Okamoto^{1*}

Division of Virology, Department of Infection and Immunity, Jichi Medical School, Tochigi-Ken,¹ Institute of Immunology, Tokyo,²
Department of Internal Medicine, Kin-ikyo Chuo Hospital, Hokkaido,³ First Department of Internal Medicine, Iwate Medical
University, Iwate-Ken,⁴ Japanese Red Cross Yamaguchi Blood Center, Yamaguchi-Ken,⁵ Masuko Memorial Hospital and
Masuko Institute for Medical Research, Aichi-Ken,⁶ Department of Internal Medicine, Iwaki Kyoritsu General
Hospital, Fukushima-Ken,⁷ and Aikawa Internal Medicine Hospital, Ibaraki-Ken,⁸ Japan

Received 3 July 2004/Returned for modification 21 September 2004/Accepted 29 September 2004

Serum samples collected from 68 patients (age, mean \pm the standard deviation [SD], 56.3 ± 12.8 years) at admission who were subsequently molecularly diagnosed as having hepatitis E and from 2,781 individuals who were assumed not to have been recently infected with hepatitis E virus (HEV; negative controls; 52.9 ± 18.9 years), were tested for immunoglobulin M (IgM) and IgA classes of antibodies to HEV (anti-HEV) by in-house solid-phase enzyme immunoassay with recombinant open reading frame 2 protein expressed in the pupae of silkworm as the antigen probe. The 68 patients with hepatitis E had both anti-HEV IgM and anti-HEV IgA. Among the 2,781 controls, 16 (0.6%) had anti-HEV IgM alone and 4 (0.1%) had anti-HEV IgA alone: these IgA/IgM anti-HEV-positive individuals were not only negative for HEV RNA but lack IgG anti-HEV antibody as well (at least in most of the cases). Periodic serum samples obtained from 15 patients with hepatitis E were tested for HEV RNA, anti-HEV IgM, and anti-HEV IgA. Although HEV RNA was detectable in the serum until 7 to 40 (21.4 ± 9.7) days after disease onset, both IgM and IgA anti-HEV antibodies were detectable until 37, 55, or 62 days after disease onset in three patients and up through the end of the observation period (50 to 144 days) in 12 patients. These results indicate that detection of anti-HEV IgA alone or along with anti-HEV IgM is useful for serological diagnosis of hepatitis E with increased specificity and longer duration of positivity than that by RNA detection.

Hepatitis E, the major form of enterically transmitted non-A, non-B hepatitis, is caused by hepatitis E virus (HEV). HEV is transmitted primarily by the fecal-oral route. Waterborne epidemics are characteristic of hepatitis E in developing regions of Africa, the Middle East, and Southeast and Central Asia, where sanitation conditions are suboptimal; one epidemic has also been documented in North America (Mexico) (32). HEV-associated hepatitis also occurs among individuals in industrialized countries with no history of travel to areas where HEV is endemic (6, 9, 18, 25, 36, 37, 39, 41, 52, 54). Recently, accumulating lines of evidence indicate that hepatitis E is a zoonosis, and pigs or other animals may act as reservoirs for HEV infection in humans (9, 15, 20–24, 27, 39, 42, 45, 56). A significant proportion of healthy individuals in industrialized countries where hepatitis E is not endemic are seropositive for HEV antibodies (8, 19, 46). Therefore, several epidemiological questions remain unanswered. The success of future studies on clinical and subclinical HEV infection not only in developing

countries but also in industrialized countries will greatly depend on the availability of assays that are sensitive and specific.

HEV was recently classified as the sole member of the genus *Hepevirus* in the family *Hepeviridae*. The genome of HEV is a 7.2-kb, positive-sense, single-stranded RNA. It contains a short 5' untranslated region, three open reading frames (ORFs; ORF1, ORF2 and ORF3), and a short 3' untranslated region terminated by a poly(A) tract (12, 34, 44, 53). ORF1 encodes nonstructural proteins, ORF2 encodes the capsid protein, and ORF3 encodes a cytoskeleton-associated phosphoprotein. Extensive diversity has been noted among HEV isolates, and HEV sequences have been classified into four major genotypes (genotypes 1 to 4) (37). In Japan, polyphyletic HEV strains of genotype 3 or 4 or both have been isolated from patients with sporadic acute or fulminant hepatitis E who had no history of travel to countries where this virus is endemic (1, 25, 30, 40, 41, 56).

The immunoglobulin M (IgM) class of antibody against HEV (anti-HEV IgM) is used as a reliable and sensitive marker of recent HEV infection (2–4, 38). However, the specificity of the solid-phase assay for anti-HEV IgM has been questioned in some cases, particularly in patients with IgM-rheumatoid factors in the serum, which have activity against the Fc portion of IgG directed to HEV antigen and may elicit

* Corresponding author. Mailing address: Division of Virology, Department of Infection and Immunity, Jichi Medical School, 3311-1 Yakushiji, Minamikawachi-Machi, Tochigi-Ken 329-0498, Japan. Phone: 81-285-58-7404. Fax: 81-285-44-1557. E-mail: hokamoto@jichi.ac.jp.